
Masters Theses

Student Theses and Dissertations

Spring 2019

Modeling impact of glass weave on differential phase skew by design of experiments method

Feng Zhang

Follow this and additional works at: https://scholarsmine.mst.edu/masters_theses



Part of the [Electrical and Computer Engineering Commons](#)

Department:

Recommended Citation

Zhang, Feng, "Modeling impact of glass weave on differential phase skew by design of experiments method" (2019). *Masters Theses*. 7897.

https://scholarsmine.mst.edu/masters_theses/7897

This thesis is brought to you by Scholars' Mine, a service of the Missouri S&T Library and Learning Resources. This work is protected by U. S. Copyright Law. Unauthorized use including reproduction for redistribution requires the permission of the copyright holder. For more information, please contact scholarsmine@mst.edu.

MODELING IMPACT OF GLASS WEAVE ON DIFFERENTIAL
PHASE SKEW BY DESIGN OF EXPERIMENTS METHOD

By

FENG ZHANG

A THESIS

Presented to the Faculty of the Graduate School of the
MISSOURI UNIVERSITY OF SCIENCE AND TECHNOLOGY

In Partial Fulfillment of the Requirements for the Degree
MASTER OF SCIENCE IN ELECTRICAL ENGINEERING

2019

Approved by

Jun Fan, Advisor
Victor Khilkevich
Mikheil Tsiklauri

© 2019
Feng Zhang
All Rights Reserved

ABSTRACT

The glass weave structure of a manufactured Printed Circuit Board (PCB) is scanned under a Scanning Electron Microscope (SEM), with top-down and cross-sectional views. Previously, analytical methods were used to investigate the glass-weave effect on transition properties in a PCB. Based on the SEM observation, this study was conducted to build full-wave models using various glass-weave types and different relative positions between differential traces and glass-weave bundles. This study aims to obtain the relationship between the glass weave and trace geometry, and the phase skew of the differential trace by using Design of Experiment (DoE) method and simulation results.

ACKNOWLEDGMENTS

I would like to express my deepest gratitude and appreciation to the following people who have been a huge part of my research study and learning journey.

To my adviser, Dr. Jun Fan, for patiently guiding me throughout my master's program. I am very grateful to him for training me on how to deal with different kinds of tough situations in academic research. I thank Dr. Jun Fan, not only for being my academic adviser, but also for being my mentor in life.

To Dr. Victor Khilkevich, for his guidance and encouragement when I was just starting out in the EMC area.

To Dr. Mikheil Tsiklauri, for helping me improve my coding skill and applying the EMC/SI theory.

To Dr. Chulsson Hwang, for his advice during my period of confusion, when I was struggling to adjust in a new area.

To Dr. David Pommerenke, for his superb skills and profound experience, which helped me to look at research problems in a new perspective.

To Dr. James Drewniak, for his efforts to effectively mentor and motivate me .

To all the faculty of the EMC Laboratory, for sharing their priceless knowledge with me.

To Bichen Chen and Shuai Jin, for their leadership in different projects.

To all my friends at the EMC Laboratory, Missouri S&T, for their advice and help throughout my master's program.

Finally, to my family and my loving wife. They never fail to show their love, guidance and support in all pursuits and endeavors.

TABLE OF CONTENTS

	Page
ABSTRACT.....	iii
ACKNOWLEDGMENTS.....	iv
LIST OF ILLUSTRATIONS.....	vii
LIST OF TABLES.....	xi
NOMENCLATURE.....	xii
 SECTION	
1. INTRODUCTION.....	1
2. FABRICATION PROCESS OF PCB DIELECTRICS.....	2
3. ORIGIN AND IMPACT OF GLASS WEAVE EFFECT.....	9
3.1. ORIGIN OF GLASS WEAVE RESONANT FREQUENCY.....	9
3.2. ORIGIN OF GLASS WEAVE TIME SKEW.....	9
3.3. GLASS WEAVE EFFECT IMPACTED.....	12
3.3.1. S-parameters.....	12
3.3.2. Eye Diagram.	16
4. REVIEW OF GLASS WEAVE EFFECT MITIGATION STRATEGIES.....	18
4.1. TRACE ROTATION.....	18
4.2. PANEL ROTATION.....	20
4.3. ZIG-ZAG ROUTING.....	22
4.4. USING LOWER DK GLASS.....	23
4.5. WEAVES WITH DIFFERENT PITCH SIZE.....	24
4.6. USING SPREAD GLASS.....	25

4.7. USING MULTI-LAYER GLASS.....	26
5. GLASS WEAVE EFFECT MEASUREMENT & FULL WAVE MODELING.....	27
5.1. TEST VEHICLE MEASUREMENT.....	27
5.1.1. Test Board Information.....	27
5.1.2. Test Vehicle Measurement Results And Analysis.....	30
5.2. FULL WAVE MODELING.....	33
5.2.1. Method Validation.....	33
5.2.2. Full Wave Simulation With Accurate Glass Bundle Model.....	42
5.2.3. Impact of Glass Weave on Jitter by DoE Method.....	44
6. CONCLUSION AND FUTURE WORK.....	50
BIBLIOGRAPHY.....	51
VITA.....	53

LIST OF ILLUSTRATIONS

	Page
Figure 2.1. PCB construction process.....	3
Figure 2.2. Glass yarn production.....	3
Figure 2.3. Glass yarn weaving process.....	4
Figure 2.4. Plain weave glass fabric: 106, 2313 and 3313.....	4
Figure 2.5. Cross-section schematic of glass weave.....	5
Figure 2.6. SEM observation on cross-section of glass type 3313.....	7
Figure 3.1. Impact of unbalanced differential lines.....	10
Figure 3.2. Differential microstrip line with different related location.....	10
Figure 3.3. Differential stripline with different related location.....	11
Figure 3.4. Fundamental differential pair transmission-line.....	12
Figure 3.5. Single-ended insertion loss (S13 & S24) and differential insertion loss (Sdd21).....	14
Figure 3.6. Phase of single-ended insertion loss (S13 & S24).....	14
Figure 3.7. Measured differential insertion loss with a dip effect by glass weave.....	15
Figure 3.8. The relationship between glass weave pitch size and wavelength.....	16
Figure 3.9. Differential signal eye diagram for transmitter (top), receiver (middle) and receiver through a big skew channel (bottom).....	17
Figure 4.1. Differential traces before rotation (left) and after rotation (right).....	18
Figure 4.2. Trace angle of rotation and glass weave pitch size.....	19
Figure 4.3. Resonant frequency with different angle of rotation for glass type 1080.....	20
Figure 4.4. Panel rotation with glass type 3313.....	21
Figure 4.5. Zig-zag routing with glass type 3313.....	22

Figure 4.6. Schematic for weaves with different pitch size.....	24
Figure 4.7. Top view for regular (left) and spread (right) glass bundle.....	25
Figure 4.8. Cross-section view for regular (left) and spread (right) glass bundle.....	25
Figure 4.9. Cross-section view for regular (left) and 2-ply (right) glass bundle.....	26
Figure 4.10. Cross-section view for 2-ply glass bundle (type 3313).....	26
Figure 5.1. Stack-up of the test vehicle.....	28
Figure 5.2. Top view of the test vehicle.....	28
Figure 5.3. Cross-section of glass bundle (left) and top view (right).....	29
Figure 5.4. Top view dimensions of the glass weave 3313.....	29
Figure 5.5. Differential insertion loss for the 4 inches trace.....	30
Figure 5.6. Differential insertion loss for the 8 inches trace.....	30
Figure 5.7. Differential insertion loss for the 12 inches trace.....	31
Figure 5.8. Sdd21 after de-embedding, 8 inches trace(top) and 12 inches trace (bottom).....	32
Figure 5.9. Phase difference after de-embedding: 8 inches trace (top) and 12 inches trace (bottom).....	32
Figure 5.10. Four types of cross-section model in Q2D.....	33
Figure 5.11. 1-ply glass weave model in HFSS.....	33
Figure 5.12. Insertion loss - pitch size 60 mil vs 120 mil.....	34
Figure 5.13. Return loss - pitch size 60 mil vs 120 mil.....	34
Figure 5.14. Insertion loss - Q2D vs HFSS.....	35
Figure 5.15. Return loss - Q2D vs HFSS.....	35
Figure 5.16. Top view of 0 degree differential trace.....	36
Figure 5.17. Single-ended insertion loss of 0 degree differential trace.....	36

Figure 5.18. Single-ended return loss of 0 degree differential trace.....	37
Figure 5.19. Differential insertion loss of 0 degree differential trace.....	37
Figure 5.20. Unwrapped phase (left) and phase difference (right) of 0 degree differential trace.....	37
Figure 5.21. Top view of the ‘worst case’ differential trace.....	38
Figure 5.22. Single-ended insertion loss of the ‘worst case’	38
Figure 5.23. Single-ended return loss of the ‘worst case’	39
Figure 5.24. Differential insertion loss of the ‘worst case’	39
Figure 5.25. Unwrapped phase (left) and phase difference (right) of the ‘worst case’	39
Figure 5.26. Top view of 5 degrees rotation differential trace.....	40
Figure 5.27. Single-ended insertion loss of 5 degrees rotation.....	40
Figure 5.28. Single-ended return loss of 5 degrees rotation.....	41
Figure 5.29. Differential insertion loss of 5 degrees rotation.....	41
Figure 5.30. Unwrapped phase (left) and phase difference (right) of 5 degrees rotation.....	41
Figure 5.31. Oval cross-section of the glass bundle model.....	42
Figure 5.32. Worst case with the oval cross-section of the glass bundle.....	43
Figure 5.33. Single-ended phase (left) and phase difference (right) of the oval cross-section of the glass bundle ‘worst case’	43
Figure 5.34. Top view and cross-section of non-bundle shift trace (left); bundle shift trace (right).....	45
Figure 5.35. Unwrapped phase (left) and phase difference (right) of non-bundle shift case.....	46
Figure 5.36. Unwrapped phase (left) and phase difference (right) of bundle shift case.....	46

Figure 5.37. Eye diagram of non-bundle shift case (left); bundle shift case (right).....	46
Figure 5.38. The angle of rotation and trace shift in DoE method.....	47
Figure 5.39. Phase difference bivariate fit by the angle of rotation.....	49

LIST OF TABLES

	Page
Table 2.1. IPC standard for fiberglass yarn nomenclature.....	6
Table 2.2. Typical dielectric material property.....	7
Table 3.1. Four port mixed mode S-parameters.....	13
Table 4.1. Properties of E-glass and NE-glass.....	23
Table 5.1. Glass weave 3313 dimensions comparison between specified and measured.....	29
Table 5.2. Phase difference vs the angle of rotation.....	48

NOMENCLATURE

<u>Symbol</u>	<u>Description</u>
DK	Dielectric constant
DF	Loss Tangent
BER	Bit error rate
PCB	Printed circuit board
SEM	Scanning electron microscope
ϵ_{eff}	Effective dielectric constant
ρ	Volume percentage of glass/resin
EM	Electromagnetic
v	Velocity of EM wave in a medium
c	Velocity of light/EM wave in free space
λ	Wave length of EM wave in a medium
ps	Picoseconds
DUT	Device under test
VNA	Vector network analyzer
DoE	Design of Experiments

1. INTRODUCTION

Some woven fiberglass fabrics are reinforced with epoxy resin. The Dielectric constant (DK) and loss tangent (DF) between fabric fiber and resin are different. As a result, when the data rate increase, the difference between DK & DF will cause more signal integrity issues. The signal propagation speed within differential pair traces leads to a bit-error-rate (BER) performance that worsens and increases EMI radiation. When frequency goes higher, the time skew between positive and negative data in a differential signal causes signal integrity problem.

2. FABRICATION PROCESS OF PCB DIELECTRICS

Fiberglass fabrics causes numerous signal integrity problems. However, fiberglass fabrics and epoxy resin substrate PCB because its composition offers cost-efficient mechanical and fire-resistant properties.

PCBs are typically constructed by creating multiple layers of laminate sheets. A laminate sheet has three basic materials, which are copper, resin, and woven glass. Initially, the resin is in a liquid state. Then, the woven glass yarn is pulled through the resin to fully saturate the cloth. After that, the glass and resin combo is heated to remove volatile elements. The resulting material is commonly known as 'prepreg layer'. If the resin is heated further, it gets cured (curing) and becomes a solid material. Then, the laminate cores are fabricated using one or more plies of prepreg layer laminated under heat and pressure between two layers of copper foil. Finally, the multilayer circuit is constructed by stacking etched laminate cores, prepreg layer, and copper foil for the outer layers. The material stack is, then, laminated under heat and pressure to fully cure the prepreg while binding all the materials together. The PCB construction process is shown in Figure 2.1.

The glass weaving process makes the dielectrics in-homogeneous material. At the very beginning, there are some marble in the form of raw glass melted in a furnace. Then, the glass yarn is made by brushing, sizing, strand forming, and winding. The glass yarn production is shown in Figure 2.2 [7].

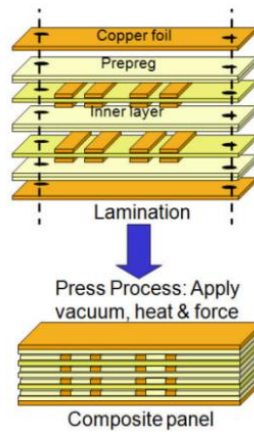


Figure 2.1. PCB construction process

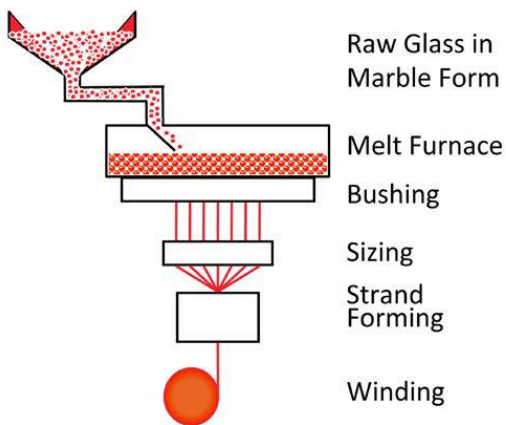


Figure 2.2. Glass yarn production

The next step is to weave the glass fiber. It is very similar with weaving the garments. The glass bundles are facing two different directions during the weaving. The glass bundles that are held tightly are called warp direction while the other kind of bundles are called weft direction. The weaving process is shown in Figure 2.3 [9].

This kind of glass fabric is called square glass fabric. There are more different glass styles like 106, 2313, 3313, 7826. They are weaved using different kinds of yarn materials. They are defined by IPC standard as shown in Table 2.1. Plain weave glass fabric is shown in Figure 2.4.

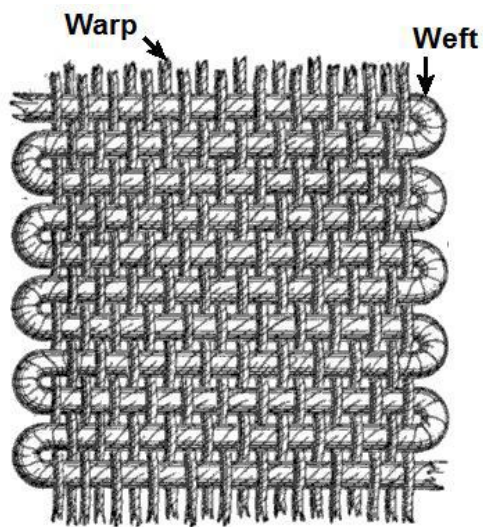


Figure 2.3. Glass yarn weaving process

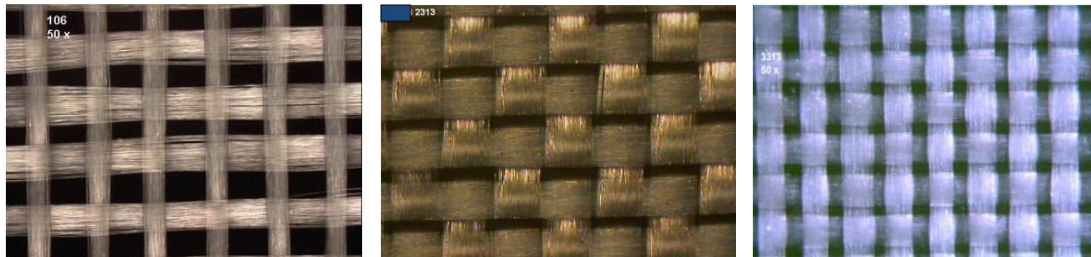


Figure 2.4. Plain weave glass fabric: 106, 2313 and 3313

The important parameters described in the cross-section schematic of glass weave is shown in Figure 2.5. The bundle thickness and pitch size are prescribed by the IPC standard is shown in Table 2.1.

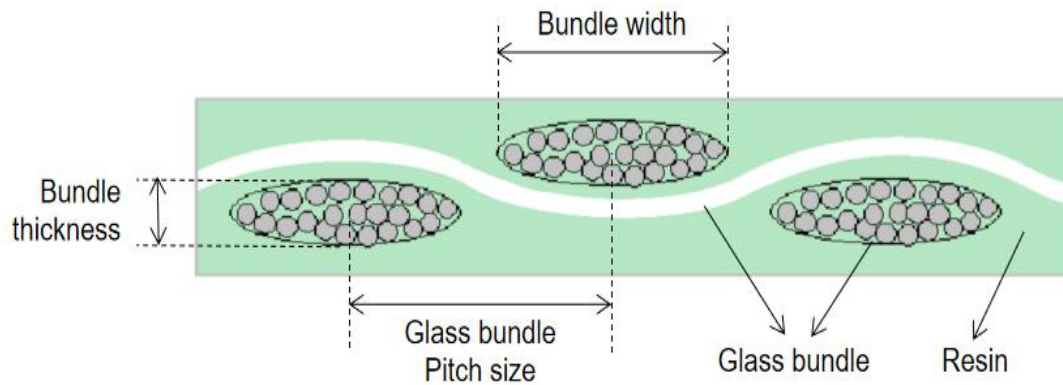


Figure 2.5. Cross-section schematic of glass weave

In the IPC standard for fiberglass yarn nomenclature, the number of glass bundles per inch along warp and weft direction are defined. The pitch size for certain glass style could be calculated by the count per inch. For example, glass type 3313 has 61 bundles per inch in warp count and 62 bundles per inch in weft count, so the glass bundle pitch size could be calculated through:

$$\text{Warp pitch} = 1000 \text{ mil} / 61 = 16.39 \text{ mil}$$

$$\text{Weft pitch} = 1000 \text{ mil} / 62 = 16.12 \text{ mil}$$

Table 2.1. IPC standard for fiberglass yarn nomenclature

Glass Style	Weave	Warp Count	Weft Count	Warp Yarn	Weft Yarn	Fabric Thickness (inches)	Fabric Thickness (mm)	Fabric Nominal Weight (g/m ²)
106	Plain	56	56	ECD 900	ECD 900	0.0013	0.032	25
1035	Plain	66	68	ECD 900	ECD 900	0.0011	0.030	30
1037	Plain	70	73	ECC 1200	ECC 1200	0.0011	0.030	23
1067	Plain	70	70	ECD 900	ECD 900	0.0014	0.035	31
1078	Plain	54	54	ECD 450	ECD 450	0.0017	0.040	48
1080	Plain	60	47	ECD 450	ECD 450	0.0021	0.064	49
1086	Plain	60	60	ECD 450	ECD 450	0.0022	0.050	54
1506	Plain	46	45	ECE 110	ECE 110	0.0056	0.140	165
1652	Plain	52	52	ECG 150	ECG 150	0.0045	0.114	142
2113	Plain	60	56	ECE 225	ECD 450	0.0031	0.074	78
2116	Plain	60	58	ECE 225	ECE 225	0.0037	0.097	109
2313	Plain	60	64	ECE 225	ECD 450	0.0033	0.080	81
3070	Plain	70	70	ECDE 300	ECDE 300	0.0034	0.086	93
3313	Plain	61	62	ECDE 300	ECDE 300	0.0033	0.081	82
7628	Plain	44	31	ECG 75	ECG 75	0.0068	0.173	203

Nevertheless, to get the detail parameters for full-wave simulation and further analysis, it's better to cut the print circuit board into a cross-section sample and use an Scanning electron microscope (SEM) to get the actual data. The cross-section view of glass type 3313 is shown in Figure 2.6.

Glass weave could attain the signal integrity problem mainly because of the dielectrics inhomogeneous. The Typical dielectric material property is shown in Table 2.2.

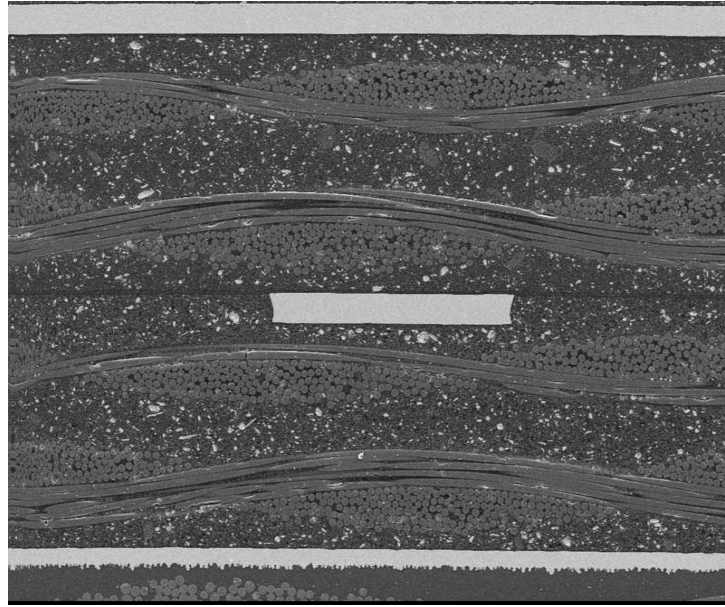


Figure 2.6. SEM observation on cross-section of glass type 3313

Table 2.2. Typical dielectric material property

Typical dielectric material property	DK	DF
Glass Weave	4.4 ~ 6.1	0.002 ~ 0.007
Resin	3.2	0.003 ~ 0.027

The effective DK is calculated by getting the average percentage volume of glass/resin and their respective DK. The following formula is widely used to calculate the effective DK of the dielectric:

$$\epsilon_{\text{reff}} = \epsilon_{\text{rglass}} * \rho_{\text{glass}} + \epsilon_{\text{rresin}} * \rho_{\text{resin}}, \quad (1)$$

where ϵ_{reff} is the effective DK of the dielectric while ϵ_{rglass} and ϵ_{rresin} are the DK of glass bundle and resin. ρ_{glass} and ρ_{resin} are the volume percentage of glass bundle and resin. The

$\mathcal{E}_{\text{reff}}$ could be used to calculate the wave speed and propagation time roughly or at low frequencies. However, when the frequency ranges to a few GHz, the in-homogeneous will become electrically small so that the dielectric could not be considered as homogeneous material any more.

3. ORIGIN AND IMPACT OF GLASS WEAVE EFFECT

3.1. ORIGIN OF GLASS WEAVE RESONANT FREQUENCY

Periodic loading on transmission lines will cause a fundamental resonance, where the distance between the discontinuities is one half of a wavelength. The harmonics of the fundamental resonance exist at higher frequencies as well [4]. In the glass weave effect, the pitch size (distance between neighboring glass bundles along the trace) will determine the fundamental resonant frequency. The periodic loading will introduce a peak in the return loss and a dip in the insertion loss at the corresponding half-wave resonant frequency.

3.2. ORIGIN OF GLASS WEAVE TIME SKEW

Differential signaling is a method of transmitting information electrically with two complementary signals sent out of two paired transmission lines.

The three advantages of using differential signaling are tolerance of ground offset, resistance to electromagnetic interference, and suitability for low-voltage electronics. Furthermore, the biggest disadvantage of differential signaling is the uneven trace length or the different signal speed that may cause time skew, which greatly affects the signal integrity. The impact of unbalanced differential lines is shown in Figure 3.1.

The dielectric in the PCB is constructed by using glass and resin. The DK value of these two materials are totally different. The effective DK as seen along the transmission line is different based on the related location between the trace and the glass bundle. The cross-section of a differential microstrip-line is shown in Figure 3.2.

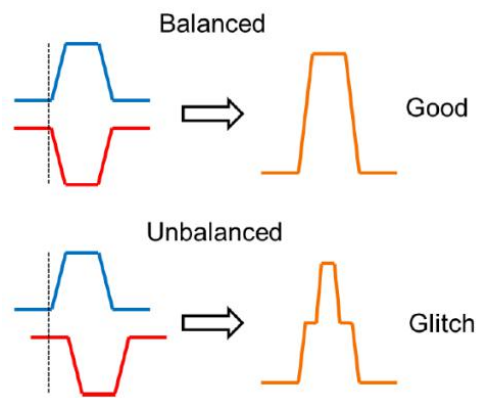


Figure 3.1. Impact of unbalanced differential lines

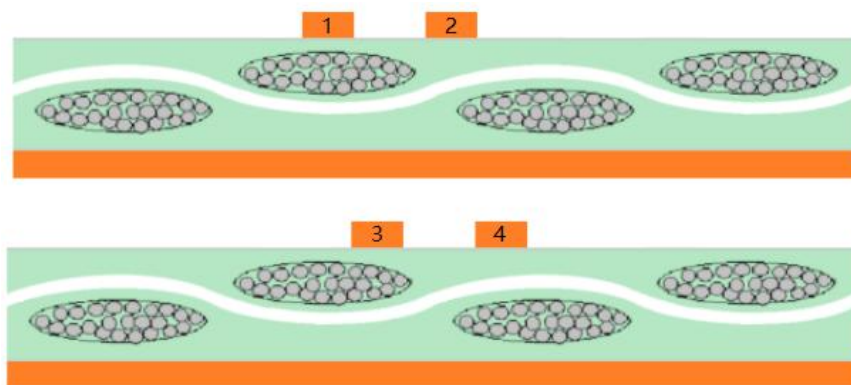


Figure 3.2. Differential microstrip line with different related location

In Figure 3.2 (top), the glass bundle is around trace 1 and trace 2 faces more resin, so the dielectric effective DK of trace 1 is higher than the dielectric effective DK of trace 2. The velocity of EM wave in a dielectric medium could be calculated through:

$$v = \frac{c}{\sqrt{\epsilon_{\text{reff}}}} \quad (2)$$

where c is the velocity of light in the free space and ϵ_{reff} is the dielectric constant (DK) of the medium. So, the velocity in trace 1 is slower than the velocity in trace 2 at this cross-section face. This will have an impact on the time skew at the end of the trace. In Figure 3.2 (bottom), the dielectric effective DK of trace 3 and 4 are more similar to each other than trace 1 and 2. The velocity should also be similar so that the time skew at the end of the differential trace is evidently smaller than top case.

The two cases in Figure 3.2 are simple situations out of many possible situations. The PCB manufacturing process could not control the relative location between the differential trace, so a method to reduce the glass weave effect will be introduced in Section 4. The comparison for differential strip line with different related location is shown in Figure 3.3.

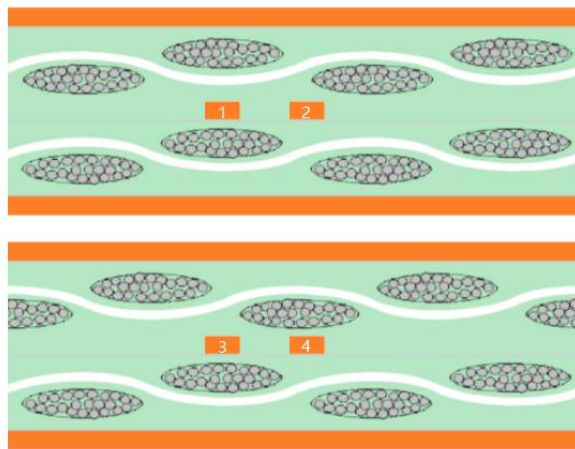


Figure 3.3. Differential strip line with different related location

When the transmission-line become complicated, as shown in Figure 3.3, the time skew at the end of the trace is dependent on both sides of the glass weave, so, if the relative location is like on the Figure 3.3 (top), it will be considered as the ‘worst case’ time skew. In real cases, the relative location is randomly placed.

3.3. GLASS WEAVE EFFECT IMPACTED

In this section how glass weave will effect the transmission-line will be analyze.

3.3.1. S-parameters. The s-parameter of transmission-line is affected by both the periodic load and the different wave velocities on various traces. A fundamental differential pair transmission-line is shown in Figure 3.4.



Figure 3.4. Fundamental differential pair transmission-line

S-parameters is combined by magnitude and phase or combined by real and imaginary part, like:

$$S_{31} = a + jb \quad (3)$$

$$S_{42} = -a - jb \quad (4)$$

The 4-port mixed mode S-parameters characterize a 4-port network in terms of the response of the network to common mode and differential stimulus signals. The 4-port mixed mode S-parameters as shown in Table 3.1.

Table 3.1. Four port mixed mode S-parameters

			Stimulus			
			Differential		Common Mode	
			Port 1	Port 2	Port 1	Port 2
Response	Differential	Port 1	SDD11	SDD12	SDC11	SDC12
		Port 2	SDD21	SDD22	SDC21	SDC22
	Common Mode	Port 1	SCD11	SCD12	SCC11	SCC12
		Port 2	SCD21	SCD22	SCC21	SCC22

The differential insertion loss could be calculated by using the signal ended s-parameters using the equation:

$$S_{dd21} = 0.5 * (S_{31} + S_{42} - S_{32} - S_{41}) \quad (5)$$

Based on Equation 5, if S_{31} and S_{42} are exactly out of phase, then, S_{dd21} will be exactly 0, so if there is a large skew between P & N signals, there will be a dip in S_{dd21} .

The dip in S_{dd21} is shown in Figure 3.5.

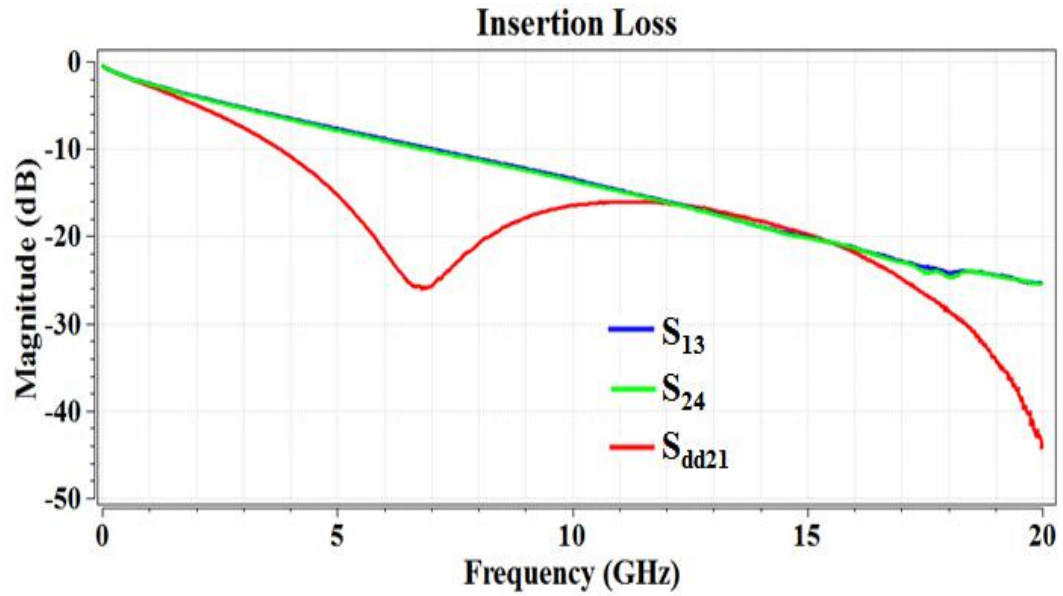


Figure 3.5. Single-ended insertion loss (S_{13} & S_{24}) and differential insertion loss (S_{dd21})

Based on the previous method, S_{13} and S_{24} should be out of phase around 6.5 GHz.

The phase difference between S_{13} & S_{24} is shown in Figure 3.6.

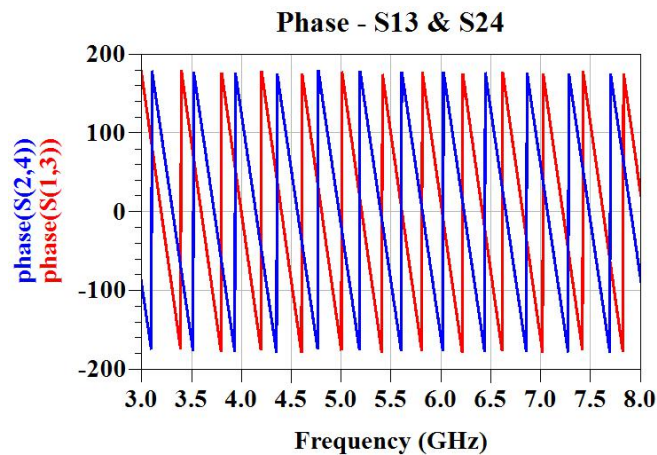


Figure 3.6. Phase of single-ended insertion loss (S_{13} & S_{24})

Figure 3.6 shows that when the differential insertion loss dips around 6.5GHz, the phase difference between the single-ended insertion loss is almost 180 degree.

Apart from the phase difference, periodic loading can also affect the insertion loss. Inhomogeneity along the line causes resonances in insertion and reflection losses.

As shown in Section 3.1, the PCB consists of two dielectric materials: resin and glass weaves. Table 2.2 shows that when going through the transmission-line (any single-ended or differential), the trace viewed as a periodic structure of glass weave embeds in a uniform material of resin. When the frequency goes to higher frequencies, the glass weave periods are electrically large, so the dielectric around the trace are inhomogeneous medium. The measured data is shown in Figure 3.7.

When the EM wave propagates in the transmission-line, and if there are periodic loading equals to a half wave length, the wavelength is satisfying the in-phase constructive. The interference will be reflected, as shown in Figure 3.8.



Figure 3.7. Measured differential insertion loss with a dip effect by glass weave

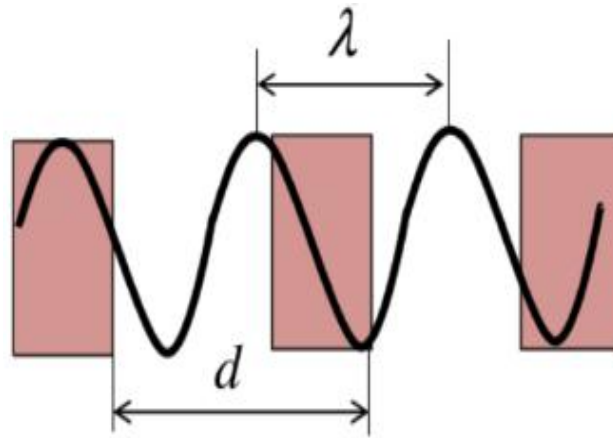


Figure 3.8. The relationship between glass weave pitch size and wavelength

Both effects may contribute to the deterministic jitter and they have to be modeled and mitigated if necessary.

3.3.2. Eye Diagram. The eye diagram of a differential signal will be closed if the differential trace become lossy because of the glass weave effect. The transmitter and receiver eye diagram are shown in Figure 3.9.

Figure 3.9 (top) shows the eye diagram of a transmitter differential signal, with a data rate of 10Gbps. After passing through a 9dB @5GHz channel, the receiver eye diagram is shown in Figure 3.9 (middle). Because of the channel loss, the eye's height and width are reduced. If the channel with the same loss become inhomogeneous because of the glass weave effect, setting the time skew between P & N traces to 80ps will completely close the eye diagram (as shown in Figure 3.9, bottom). Thus, it is very important to reduce the time skew between P & N traces.

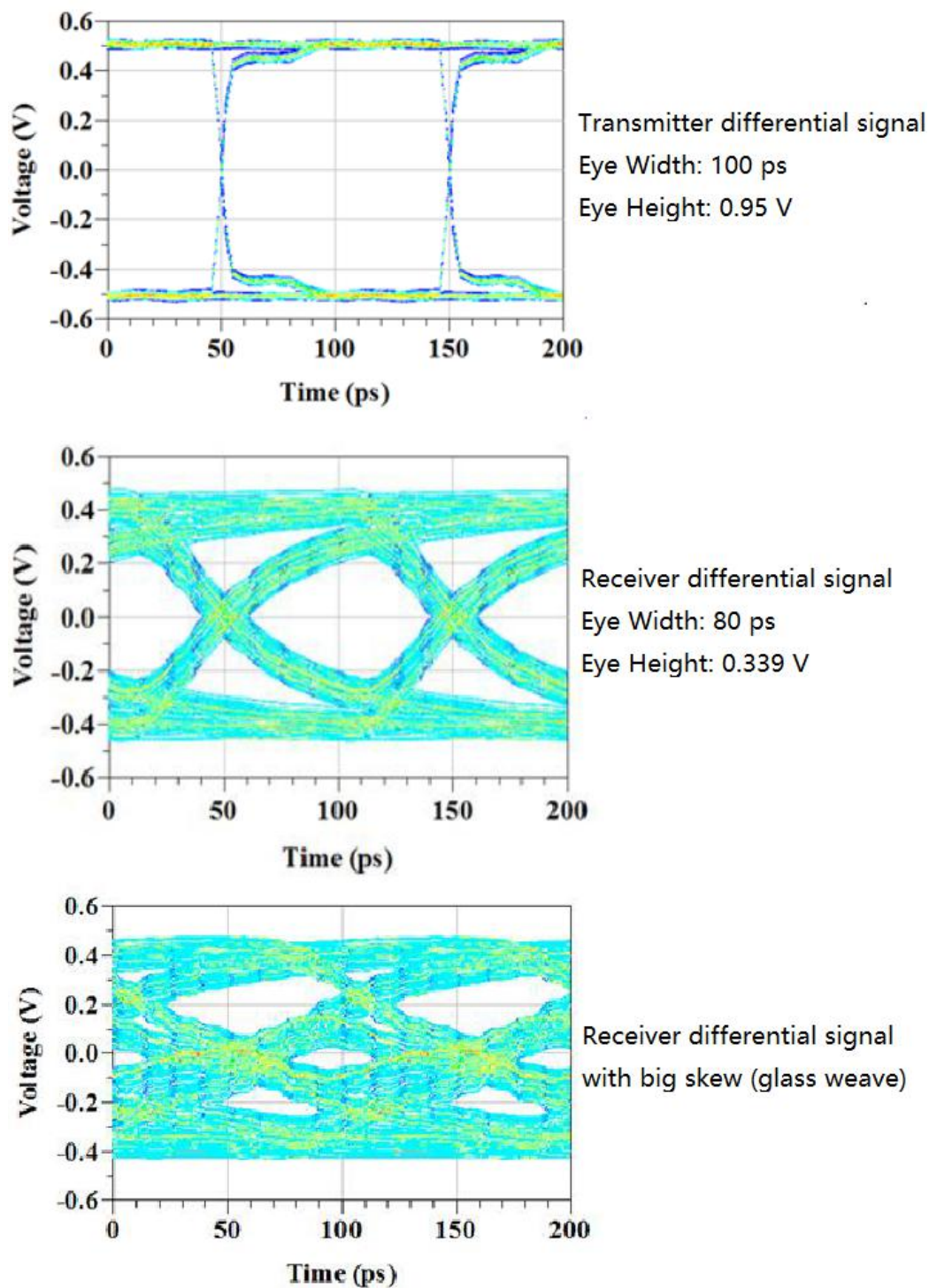


Figure 3.9. Differential signal eye diagram for transmitter (top), receiver (middle) and receiver through a big skew channel (bottom)

4. REVIEW OF GLASS WEAVE EFFECT MITIGATION STRATEGIES

There are several strategies provided by previous studies. The review and analysis for these strategies are presented in this section.

4.1. TRACE ROTATION

The time skew between differential transmission lines could be reduced by rotating the trace to a certain angle. The manufacturer could not control the relative location between the glass bundle and the trace. However, the simplest way to avoid the worst case (one trace on the glass bundle, another trace on the resin) is to rotate the trace. The differential transmission line before and after rotation is shown in Figure 4.1.

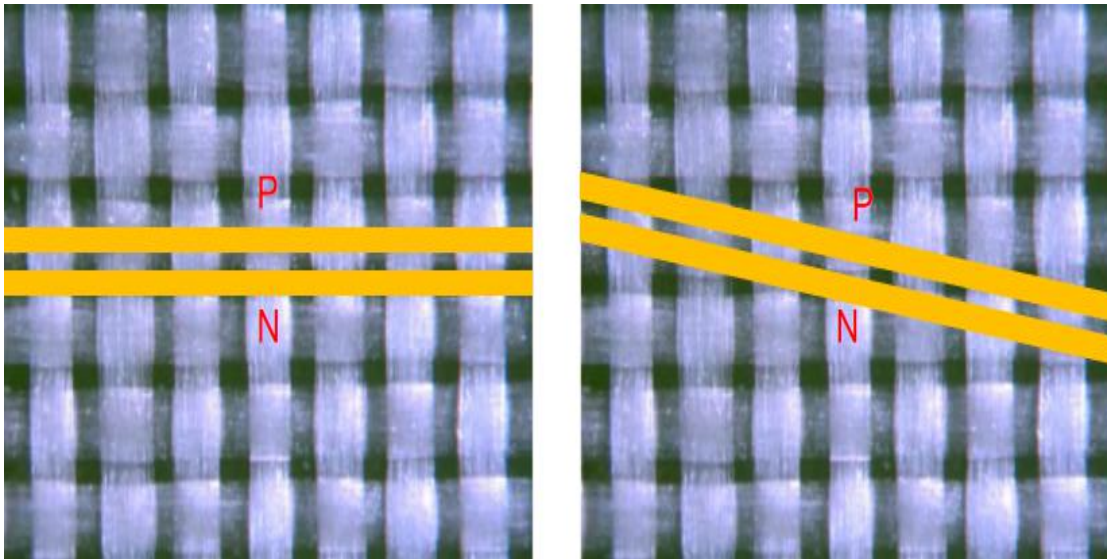


Figure 4.1. Differential traces before rotation (left) and after rotation (right)

Trace rotation can reduce the differences in the phase between P and N traces. Yet, trace rotation could not reduce the dip in insertion loss that is affected by periodic loading. A previous study [6] indicated that the first resonant frequency could be estimated by applying the formula:

$$f_{res} = \frac{c * \cos \phi}{2d \sqrt{\epsilon_{reff}}} \quad (6)$$

where c is the velocity of light in the free space, ϵ_{reff} is the dielectric constant (DK) of the medium, d is the glass weave pitch size, and ϕ is the angle between the trace and the glass bundle. Glass weave pitch size and the angle of rotation is shown in Figure 4.2.

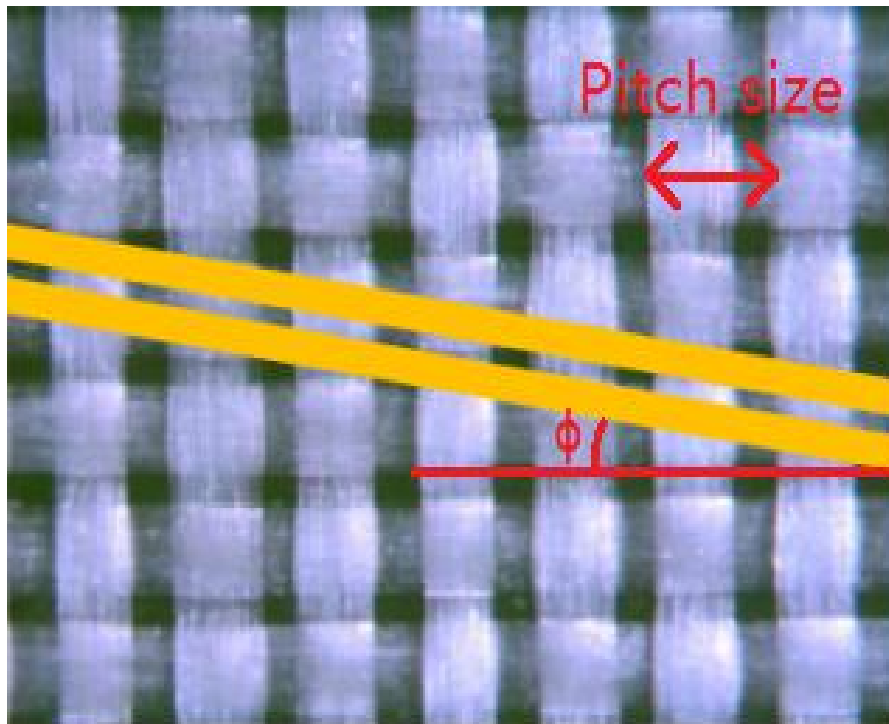


Figure 4.2. Trace angle of rotation and glass weave pitch size

The angle of rotation ϕ should be less than 45 degree. In a real-life scenario, the horizontal and vertical pitch sizes of the glass weave are slightly different (see Table 2.1). However, there are actually both horizontal resonant frequencies and vertical resonant frequencies, and the one with the sharp angle of rotation dominates the other. The resonant frequency with different angles of rotation is shown in Figure 4.3.

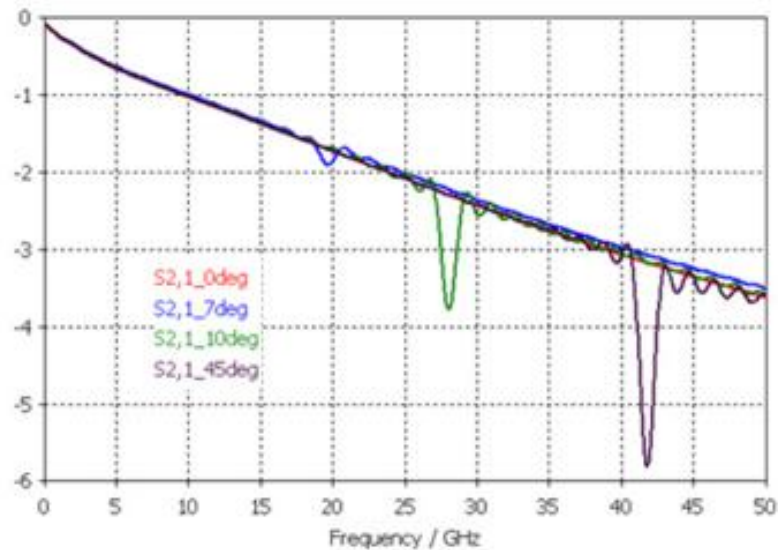


Figure 4.3. Resonant frequency with different angle of rotation for glass type 1080

4.2. PANEL ROTATION

The disadvantage of trace rotation is the space it requires. Rotating the trace will definitely increase the space requirements, thus, also increasing the cost. Moreover, if the trace is between two ASICs and the two ASICs are located at the same height on the board layout, then rotating the trace is impossible.

When the traces could not be rotated, the panel could be rotated with the glass bundle, and the excess material must be cut off the board. Furthermore, the glass bundle could be rotated while cutting into the board panel. Panel rotation has the same effect as trace rotation in terms of the signal integrity. Although they are both rotate the same position between the trace and the panel.

Figure 4.4 shows that how the extra materials are cut by using the panel rotation method, the resin and glass bundle inside the red block will contain as the dielectric in the print circuit board, all the other resin and glass bundle will be cut off the print circuit board.

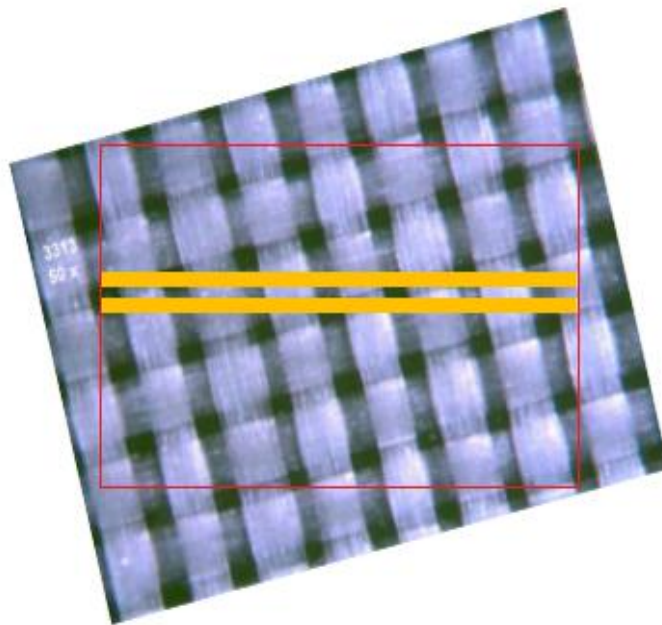


Figure 4.4. Panel rotation with glass type 3313

4.3. ZIG-ZAG ROUTING

When the space and cost do not allow the panel to rotate or the trace to directly rotate, but still wants to reduce the phase skew between the two differential traces, zig-zag routing is the best option (as shown in Figure 4.5).

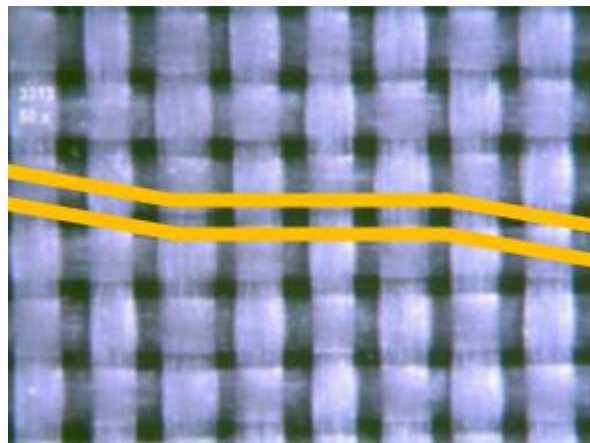


Figure 4.5. Zig-zag routing with glass type 3313

The trace could be routed so that it traverses a minimum of three times the pitch size of a fiber glass before reversing the direction of the routing. That is also one of the reasons most manufacturers choose a 10 degree rotation for both trace rotation and zig-zag rotation. In fact, it does not take much of an angle between the trace and glass bundle to resolve the fiber weave problem. The trace has to merely cross at least two glass bundles along its length so that the effect on the two adjacent trace is equalized.

4.4. USING LOWER DK GLASS

The DK difference between standard glass (DK ~ 6) and resin (DK~3.2) is the main reason for the periodic loading and phase skew. Hence, one solution to undermine the glass weave effects is to reduce the DK difference between the glass and the resin by using the low DK glass material.

One type of the lower DK glass is the NE-glass from the original E-glass. The difference between the properties of the E-glass and NE-glass is shown in Table 4.1.

Table 4.1. Properties of E-glass and NE-glass

Property	Unit	E-glass	NE-glass
Density	g/cm ³	2.6	2.3
Tensile Strength	GPa	3.2	3.1
Tensile Modulus	GPa	75	64
Dielectric constant	(1GHz)	6.8	4.8
Dissipation factor	(1GHz)	0.0035	0.0015
Volume Resistance	Ω cm	10 ¹⁵	10 ¹⁵
Specific Heat	J/kg K	863	862
Thermal Expansion	ppm/°C	5.6	3.3
The Point softening	°C	844	-

As shown in Table 4.1, both dielectric constant and dissipation factor for NE-glass is smaller than the regular type, which is the E-glass. Beside NE-glass, some manufacturers offer ultra-low DK glass (DK ~ 3.5), that is very similar to resin. However, the cost for this will also be higher than that of the regular glass.

4.5. WEAVES WITH DIFFERENT PITCH SIZE

This method is applicable only to strip-line traces. It is applied to use two different glass types with a significant pitch size difference for top and bottom substrates, to find the average of the glass weave effect. The schematic diagram for this method is shown in Figure 4.6.

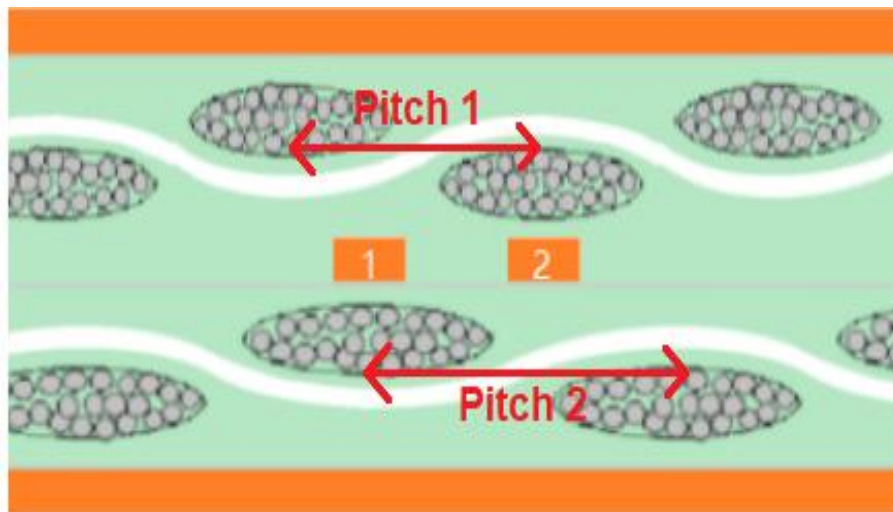


Figure 4.6. Schematic for weaves with different pitch size

Using different glass type could reduce the glass weave effect based on the periodic loading. The limitation for this method is that even though the magnitude for the dip in insertion loss will be reduce, several smaller dips will be produced because of the different pitch sizes of glass.

4.6. USING SPREAD GLASS

The gap between glass bundles mainly causes inhomogeneity. Specifying a denser weave compared to a sparse weave is an effective way to eliminate the gap between glass bundles. This will effectively reduce the phase skew. The top and cross-section view for regular glass and spread glass are shown in Figure 4.7 and Figure 4.8.

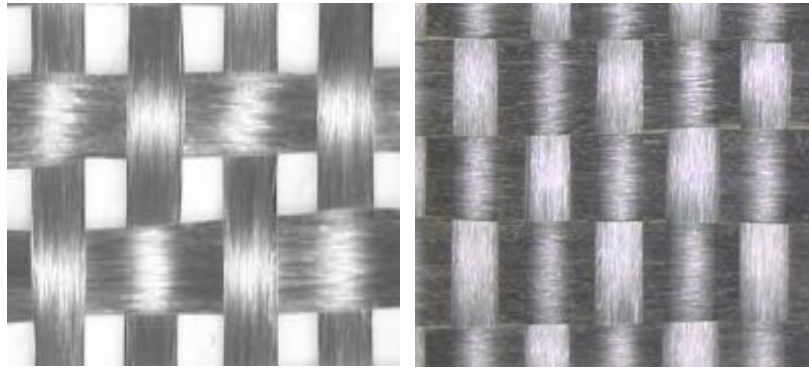


Figure 4.7. Top view for regular (left) and spread (right) glass bundle

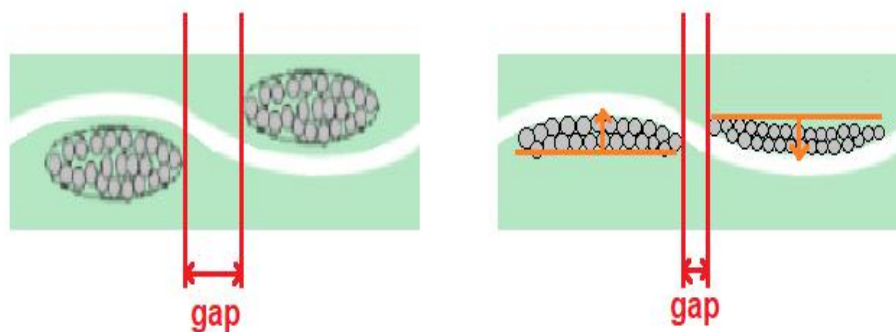


Figure 4.8. Cross-section view for regular (left) and spread (right) glass bundle

4.7. USING MULTI-LAYER GLASS

The phase skew between differential traces could be mitigated by using the averaging effect when multiple plies of glass weaves are used. The cross-section for 1-ply and 2-ply strip-line are shown in Figure 4.9.

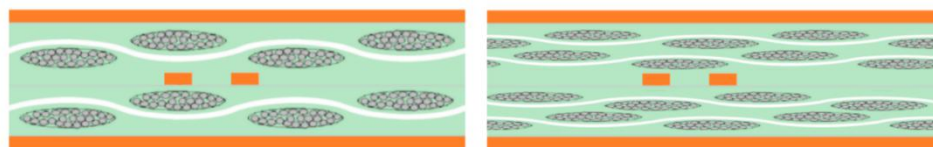


Figure 4.9. Cross-section view for regular (left) and 2-ply (right) glass bundle

Figure 4.9 (right) shows the ‘worst case’ that will only occur when all four layers have gaps that line up in the same location. Most of the time, the gap in the glass weave could be covered by neighboring layers. The cross-section view for glass type 3313 in the real case is shown as Figure 4.10.

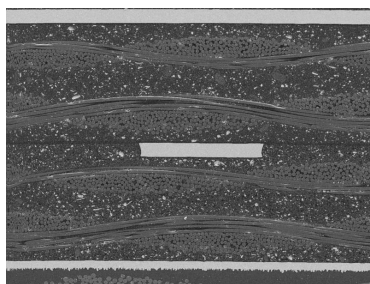


Figure 4.10. Cross-section view for 2-ply glass bundle (type 3313)

5. GLASS WEAVE EFFECT MEASUREMENT & FULL WAVE MODELING

5.1 TEST VEHICLE MEASUREMENT

In this study, the simulation modeling goes back to the simplest case to validate the model first, then use the real case parameters observed by SEM (Scanning electron microscope). Since the focus of this study is to find out the impact regularity of differential phase skew based on the glass weave effect, full wave modeling is chosen. However, the glass weave model is simplified because of the simulation time and computational resources.

5.1.1. Test Board Information. The test vehicle is Cisco SI 28G TV Test CARD REV2. 5 degrees rotation, a 16-layer test board. The traces measured in this study are 4 inches, 8 inches, and 12 inches differential strip-line on layer 12. The glass type dimensions such as bundle thickness, pitch size, and bundle width are preset by the IPC standard as shown in Table. 2.1. The other parameters which are not specified in this table could be obtained from the top view and cross-section observation. The stack-up for this test vehicle is shown in Figure 5.1 and the overall view of the test vehicle is shown in Figure 5.2.

According to Figure 5.1, one side of the trace is a 1-ply 3313 glass and the other side is a 2-ply 3313 glass. The whole board has a 5 degrees rotation. The cross-section of the differential trace and top view of the glass bundle are shown in Figure 5.3.

The glass bundle dimensions are shown in Table 5.1; and the definition of the dimensions are shown in Figure 5.3 (left) and Figure 5.4.

Type	Material Const.	Drill	Fill	Type	Thk	Er	Zo	Line	Zo	Line	Zo	Line	Space	Line
		1.7		SIM	.5	3.70								
TU872SLK	38oz (216255%)	1		Pl	1.68		50.5	8.30						
TU872SLK	1	2		Pl	.95									
TU872SLK	0.004 3313 RTF	2		Core	4.00	3.50								
TU872SLK	1	3		Pl	1.20		50.5	4.45			99.8	4.10	7.90	4.10
TU872SLK	(20331956%)	3		Core	4.00	3.50								
TU872SLK	1	4		Pl	1.20									
TU872SLK	0.004 3313 RTF	4		Core	4.00	3.50								
TU872SLK	1	5		Pl	1.20		50.5	4.45						
TU872SLK	(20331956%)	5		Core	4.00	3.50								
TU872SLK	1	6		Pl	1.20									
TU872SLK	0.004 3313 RTF	6		Core	4.00	3.50								
TU872SLK	1	7		Pl	1.20						100.2	4.40	7.60	4.40
TU872SLK	(20331956%)	7		Core	4.00	3.50								
TU872SLK	0.024 (51216 RTF	8		Pl	1.20		50.5	5.95	55.5	4.80	100.2	4.40	7.60	4.40
TU872SLK	(20331956%)	8		Core	4.00	3.50								
TU872SLK	1	9		Pl	1.20									
TU872SLK	(20331956%)	9		Core	4.00	3.50								
TU872SLK	1	10		Pl	1.20						99.8	4.10	7.90	4.10
TU872SLK	0.004 3313 RTF	10		Core	4.00	3.50								
TU872SLK	(20331956%)	10		Pl	1.20									
TU872SLK	1	11		Pl	1.20									
TU872SLK	(20331956%)	11		Core	4.00	3.50								
TU872SLK	1	12		Pl	1.20		50.5	4.45	55.3	3.60	99.8	4.10	7.90	4.10
TU872SLK	0.004 3313 RTF	12		Core	4.00	3.50								
TU872SLK	1	13		Pl	1.20									
TU872SLK	(20331956%)	13		Core	4.00	3.50								
TU872SLK	38oz	14		Pl	1.68		50.5	8.30						
		1.7		SIM	.5	3.70								

Figure 5.1. Stack-up of the test vehicle

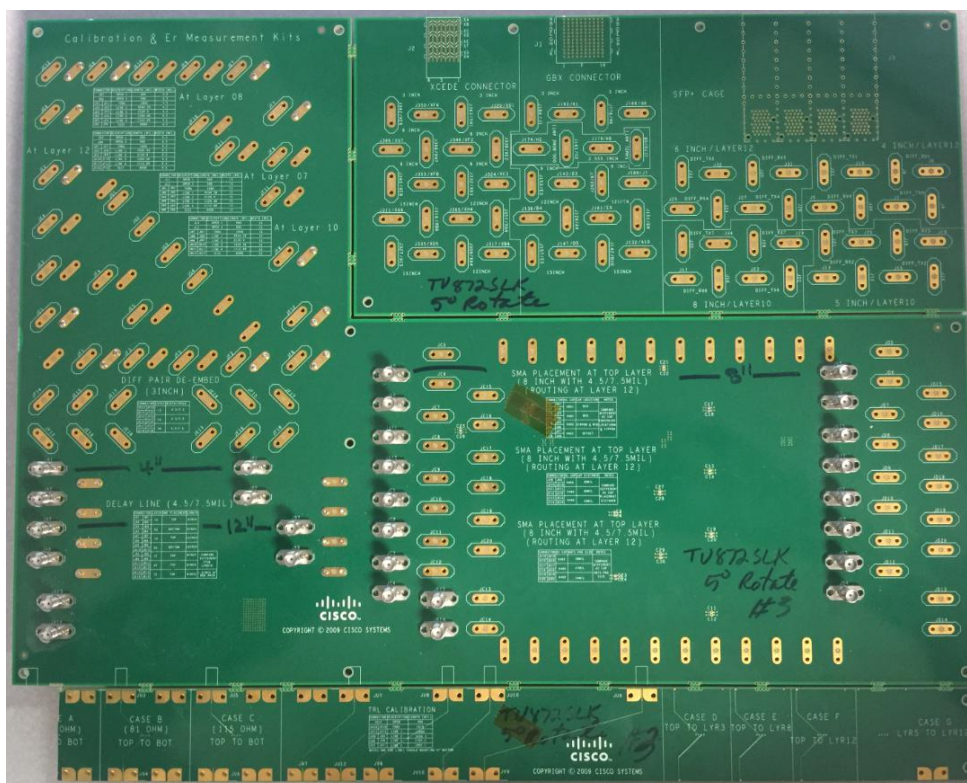


Figure 5.2. Top view of the test vehicle

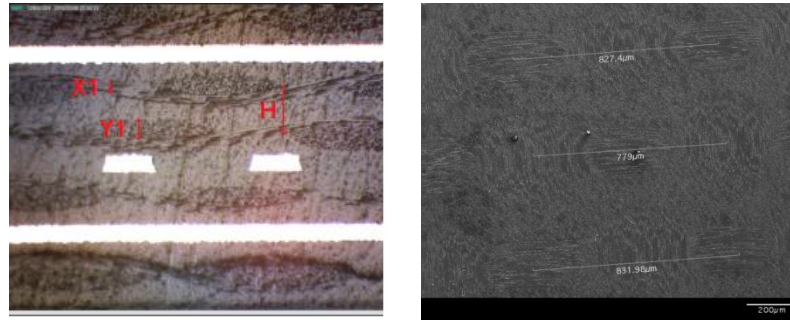


Figure 5.3. Cross-section of glass bundle (left) and top view (right)

Table 5.1. Glass weave 3313 dimensions comparison between specified and measured

Dimension(mil)	H	X1	X2	X3	Y1	Y2	Y3
Specified	4.6	1.9	13.1	16.2	1.5	11.0	16.3
Measured	4.4	1.7	13.0	16.0	1.4	11.6	16.0

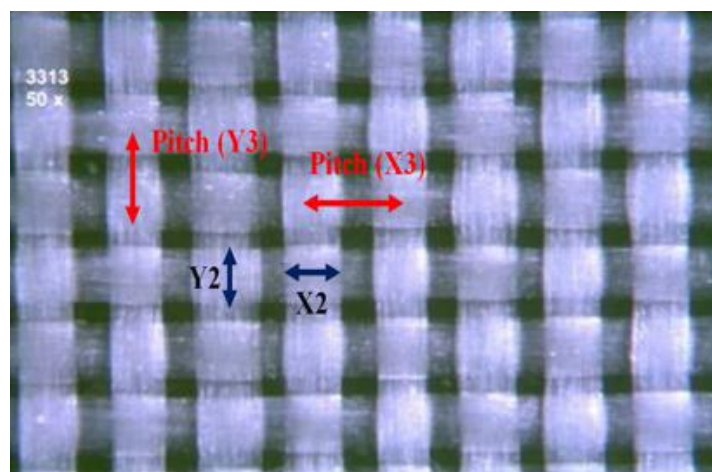


Figure 5.4. Top view dimensions of the glass weave 3313

5.1.2. Test Vehicle Measurement Results And Analysis. Parameters were measured for traces in the same layer (layer 12) in the test vehicle. The lengths are 4 inches, 8 inches, and 12 inches respectively. The differential insertion loss S_{dd21} for these are shown in Figure 5.5, Figure 5.6, and Figure 5.7.



Figure 5.5. Differential insertion loss for the 4 inches trace



Figure 5.6. Differential insertion loss for the 8 inches trace



Figure 5.7. Differential insertion loss for the 12 inches trace

The noise at the very high frequency is caused by the frequency limitation of adapter and cable. Besides, there is still a dip around 16 GHz in 8 inches and 12 inches case. To make sure that this dip is not because of the calibration / connector / via issue, the s-parameter for 4 inches trace has been used as a fixture in de-embedding the 8 inches and 12 inches traces. The de-embedding method choosed here is the Smart de-embedding, by using this type of de-embedding, it's more easy to find out where is the problem, the results will show that if the dip about 16 GHz is because of glass weave effect or not. The differential insertion loss and phase difference after de-embedding are shown in Figure 5.8 and Figure 5.9.

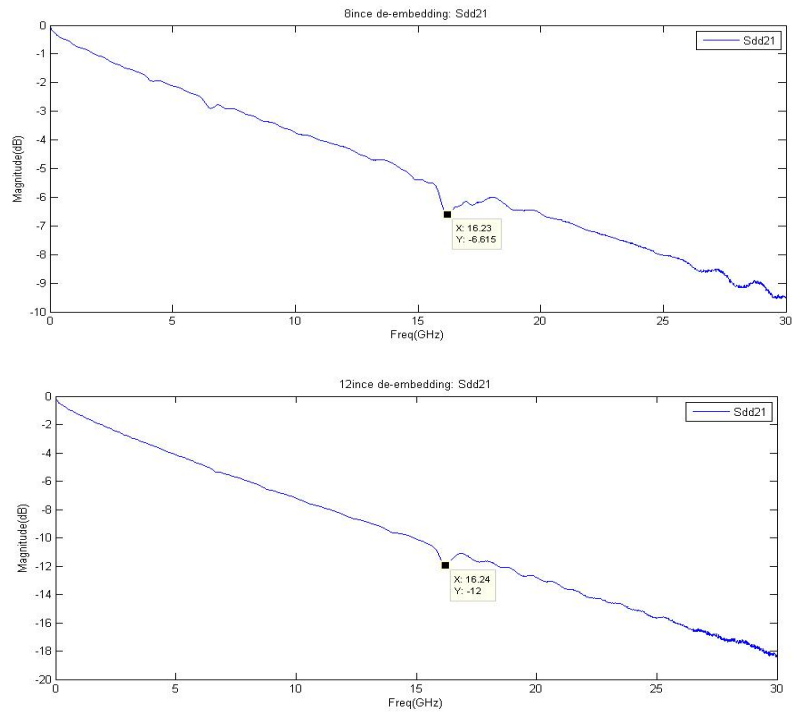


Figure 5.8. Sdd21 after de-embedding, 8 inches trace(top) and 12 inches trace(bottom)

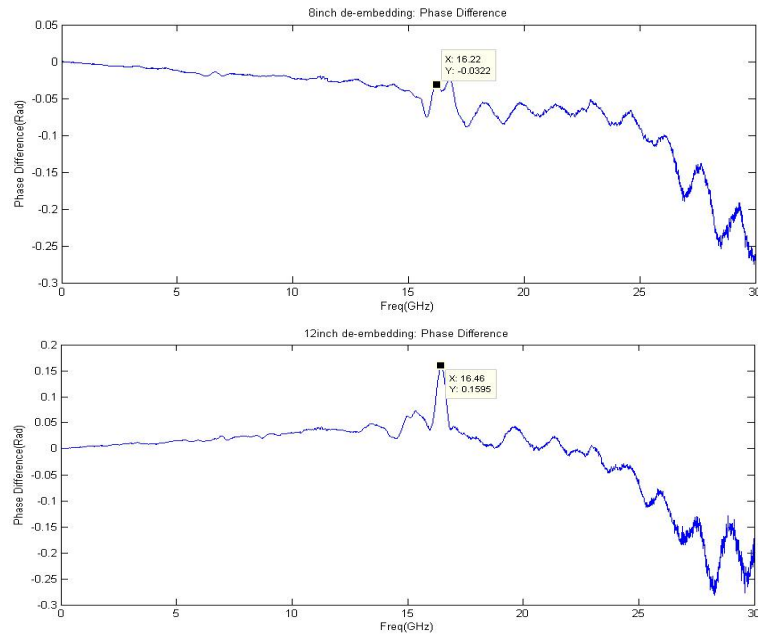


Figure 5.9. Phase difference after de-embedding: 8 inches trace (top) and 12 inches trace (bottom)

5.2. FULL WAVE MODELING

Before executing the full wave modeling for the glass weave structure, it is vital to validate the reliability and feasibility of the full wave model first. The first step is to validate the simplest structure.

5.2.1. Method Validation. A comparison between Q2D and HFSS were simulated. Four kinds of cross-section model were made in Q2d (as shown in Figure 5.10). Using these four types of cross-section cascade together, the same structure to compare with HFSS model in Figure 5.11 could be built.

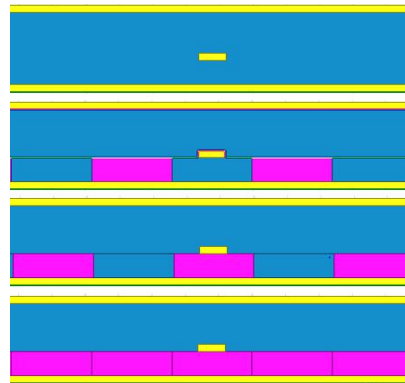


Figure 5.10. Four types of cross-section model in Q2D

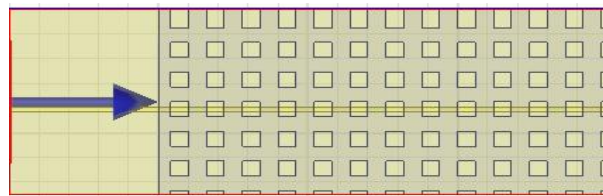


Figure 5.11. 1-ply glass weave model in HFSS

The parameters in both Q2D and HFSS models are from the test vehicle SEM observation. Additionally, a single-ended trace and only one glass weave layer were built in this model to verify if the square glass weave could mimic the glass weave effect. The comparison results for Q2D, two different pitch sizes were simulated to compare with formula 6 to see if the resonant frequency is the same. The insertion loss and return loss comparison are shown in Figure 5.12 and Figure 5.13.

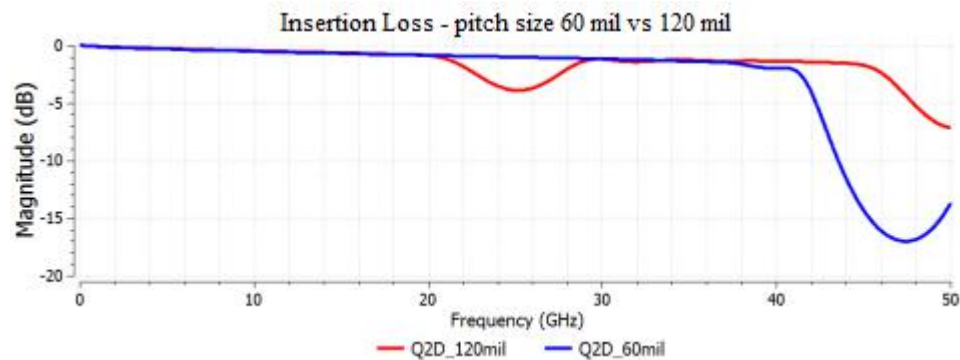


Figure 5.12. Insertion loss - pitch size 60 mil vs 120 mil

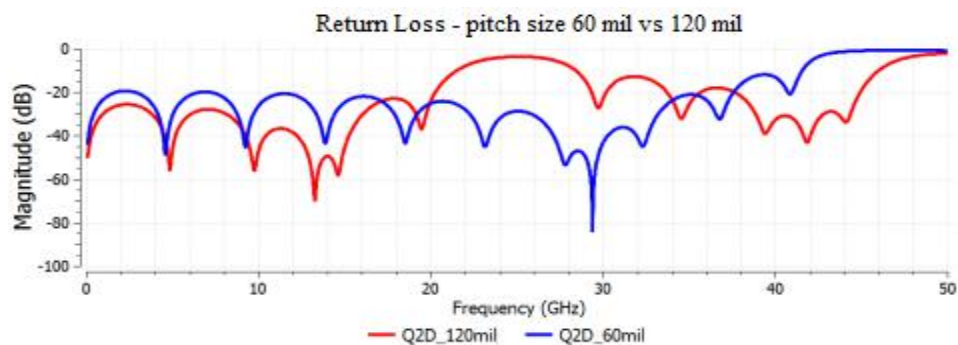


Figure 5.13. Return loss - pitch size 60 mil vs 120 mil

The total length of the differential trace is 600 mil. It is long enough to observe the glass weave effect resonant frequency. Furthermore, the resonant frequency for 60 mil pitch size and 120 mil pitch size are very similar with the resonant frequency calculated by formula (6): 24 GHz and 48 GHz. The s-parameters comparison between HFSS and Q2D for 60 mil pitch size are shown in Figure 5.14 and Figure 5.15.

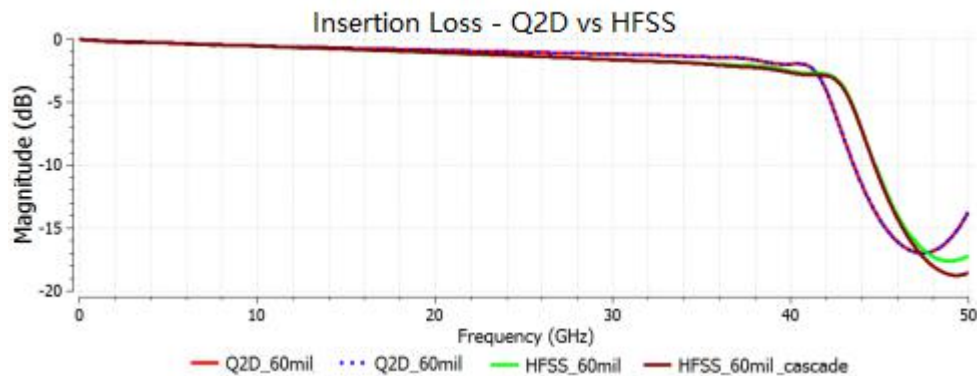


Figure 5.14. Insertion loss - Q2D vs HFSS

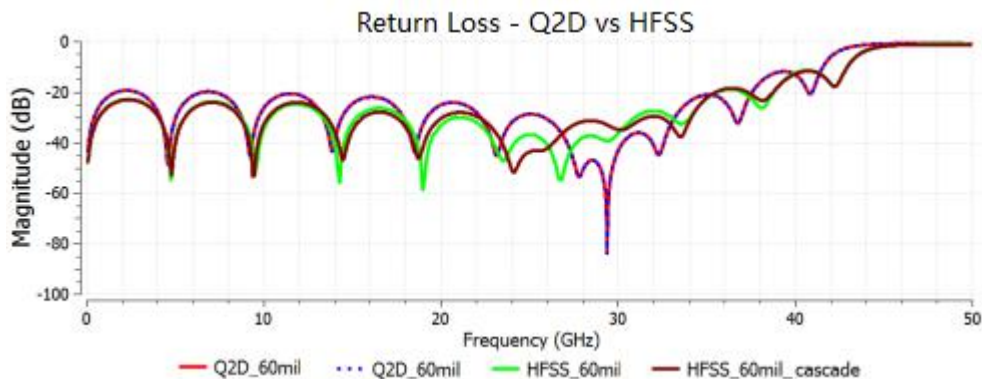


Figure 5.15. Return loss - Q2D vs HFSS

There are two HFSS models. Both of them have 60 mil pitch size of glass weave. One is a full wave model with 600 mil length while the other one is cascaded from 300 mil case. Since the difference in the cascaded model and full wave model is very small and the resonant frequency are the same, the s-parameters of shorter trace could be cascaded to get s-parameters of a longer trace to save time.

After validating the single-ended model, a differential trace model was built. The top view of the model and S-parameters results are shown in Figure 5.16, Figure 5.17, Figure 5.18, Figure 5.19, and Figure 5.20.

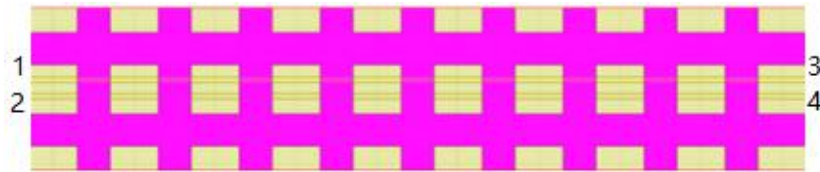


Figure 5.16. Top view of 0 degree differential trace

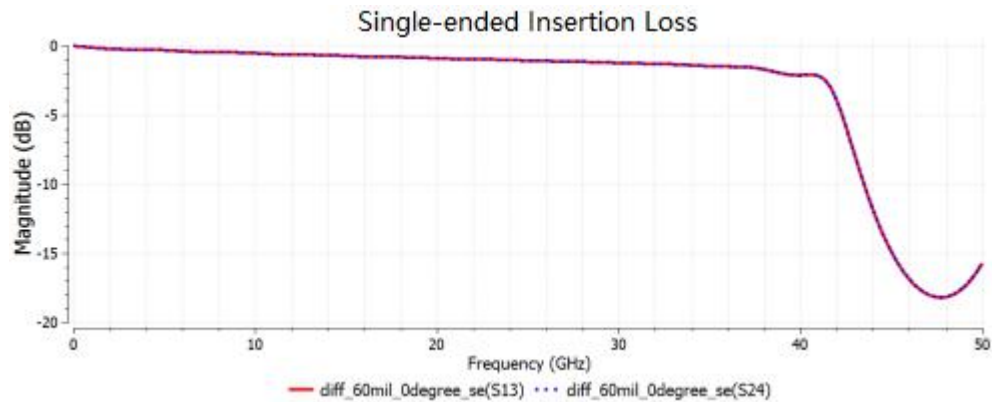


Figure 5.17. Single-ended insertion loss of 0 degree differential trace

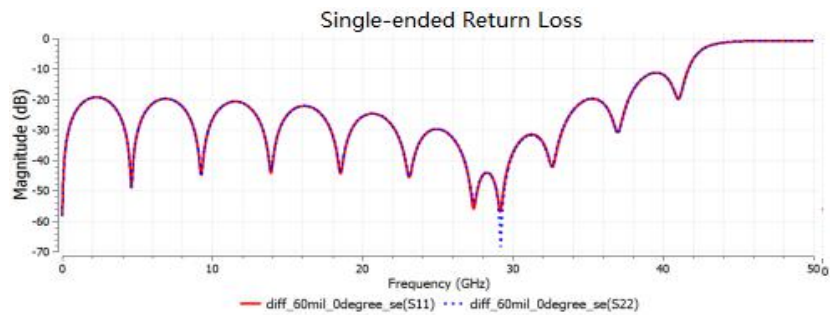


Figure 5.18. Single-ended return loss of 0 degree differential trace

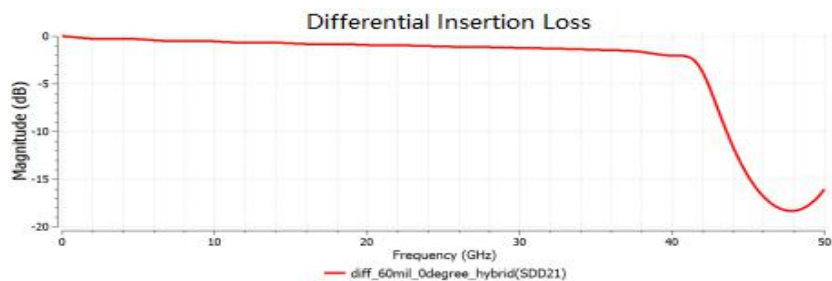


Figure 5.19. Differential insertion loss of 0 degree differential trace

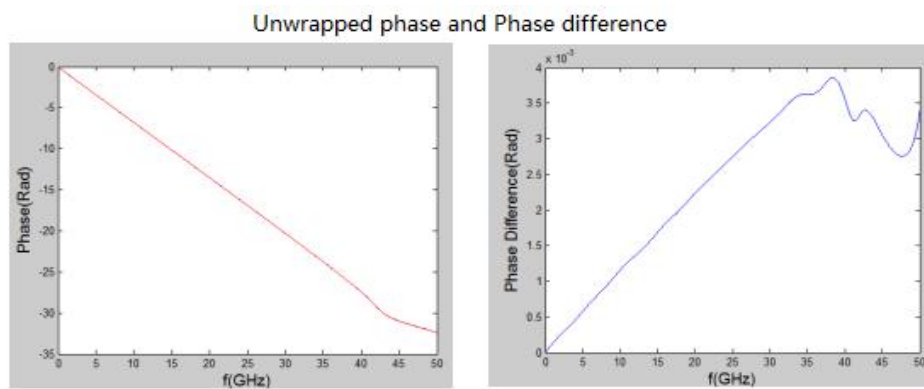


Figure 5.20. Unwrapped phase (left) and phase difference (right) of 0 degree differential trace

The P & N traces are in the same situation as the previous single-ended case so that the single-ended insertion loss and return loss are the same as the previous one. Additionally, there is almost no phase difference (0.0034 rad @ 50 GHz).

The model and results for the worst case—one trace is on the bundle while the other trace on the resin —are shown in Figure 5.21, Figure 5.22, Figure 5.23, Figure 5.24, and Figure 5.25.

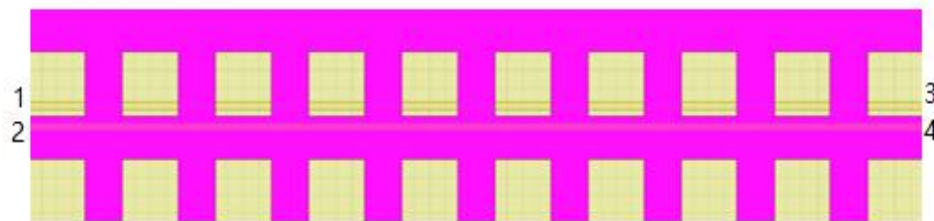


Figure 5.21. Top view of the 'worst case' differential trace

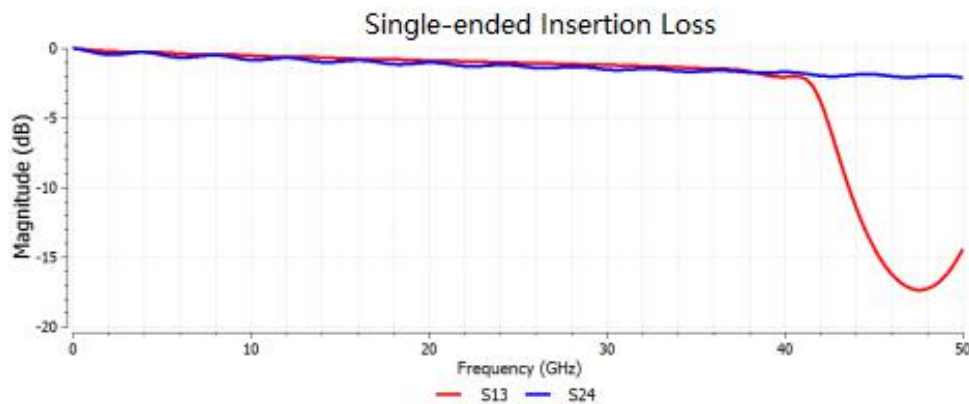


Figure 5.22. Single-ended insertion loss of the 'worst case'

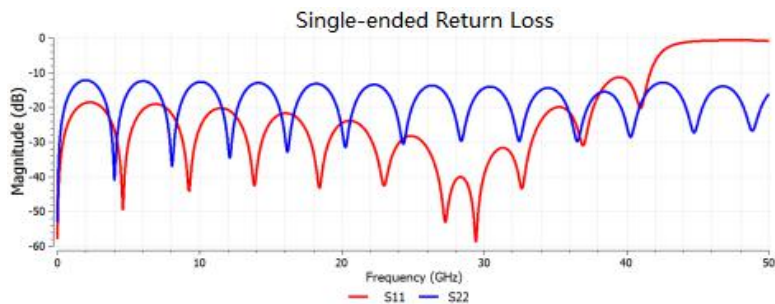


Figure 5.23. Single-ended return loss of the ‘worst case’

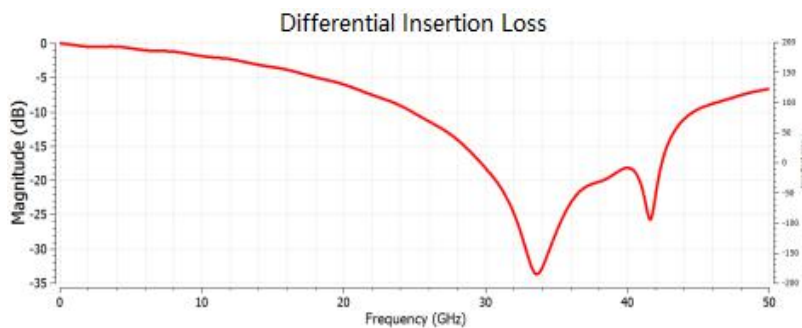


Figure 5.24. Differential insertion loss of the ‘worst case’

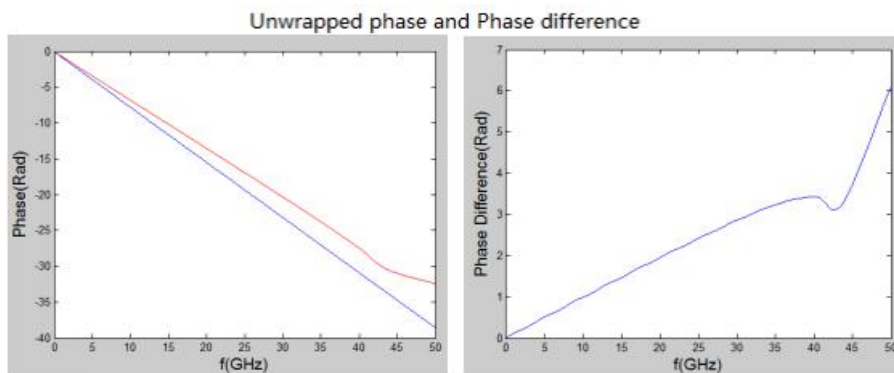


Figure 5.25. Unwrapped phase (left) and phase difference (right) of the ‘worst case’

Because this is the worst case, the phase difference between the first trace on the glass bundle and the other trace that is on the resin is pretty huge (6 rad @ 50GHz).

The 'worst case' full wave model shows that the glass bundle has a 5 degrees rotation. The top view and simulation results are shown in Figure 5.26, Figure 5.27, Figure 5.28, Figure 5.29, and Figure 5.30.

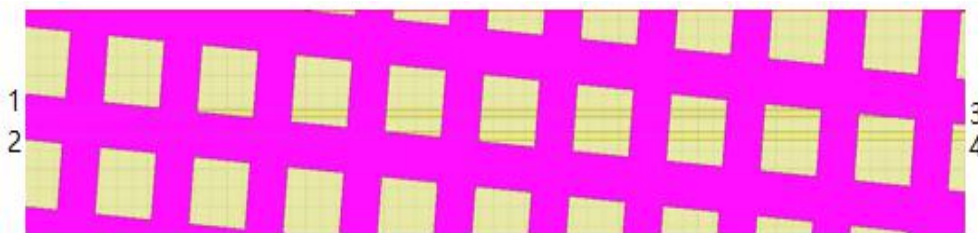


Figure 5.26. Top view of 5 degrees rotation differential trace



Figure 5.27. Single-ended insertion loss of 5 degrees rotation

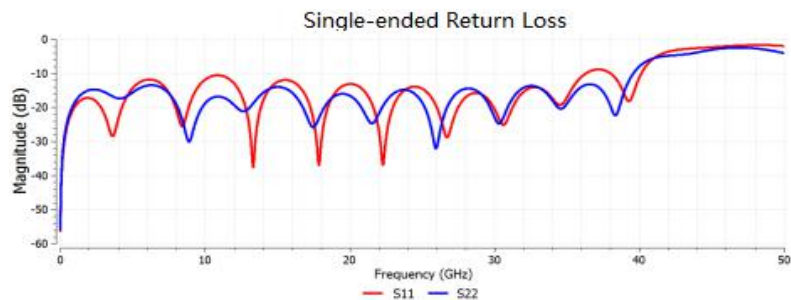


Figure 5.28. Single-ended return loss of 5 degrees rotation

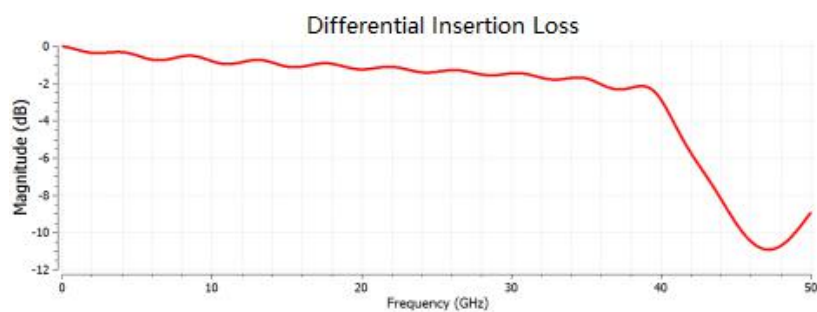


Figure 5.29. Differential insertion loss of 5 degrees rotation

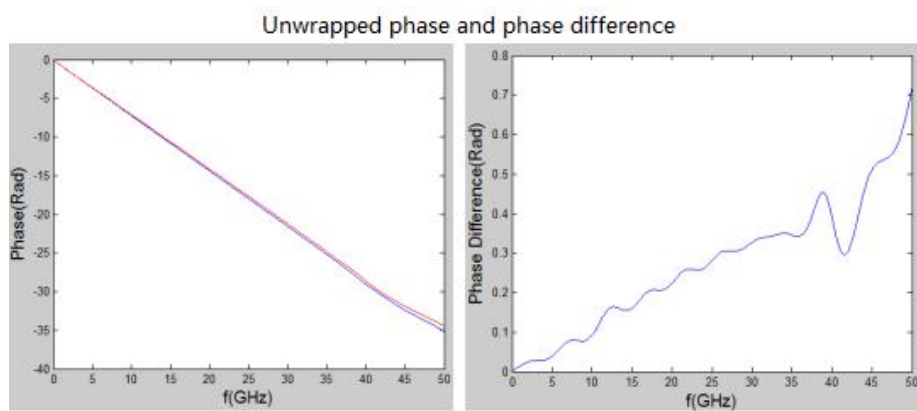


Figure 5.30. Unwrapped phase (left) and phase difference (right) of 5 degrees rotation

After the 5 degrees rotation, the time skew between P & N traces have been reduced from 6 rad to 0.7 rad at 50 GHz.

5.2.2. Full Wave Simulation With Accurate Glass Bundle Model. An oval cross-section glass bundle was built in the full weave model. The glass bundle model is shown in Figure 5.31.

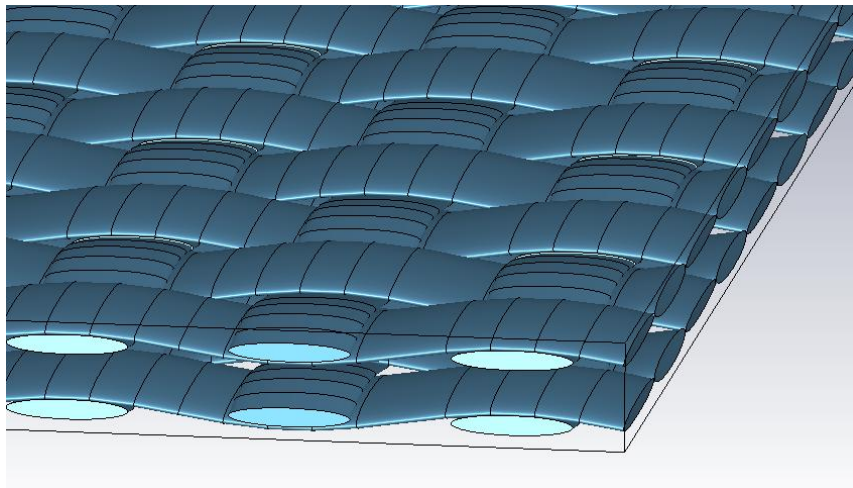


Figure 5.31. Oval cross-section of the glass bundle model

The ‘worst case’ with the oval cross-section of the glass bundle is shown in Figure 5.32. One trace is on the bundle while the other trace is on the resin. S-parameters are ignored in this case. The researchers focused on the time skew. The trace length is reduced to 300mil because of the cost of simulation time and calculation resource. The single-ended phase and phase difference are shown in Figure 5.33.

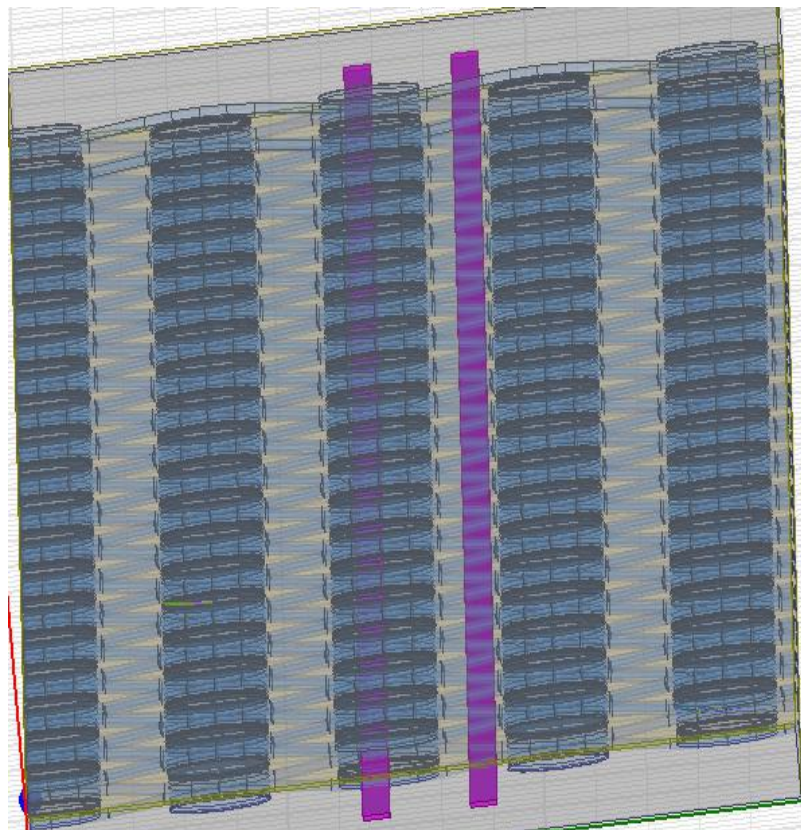


Figure 5.32. Worst case with the oval cross-section of the glass bundle

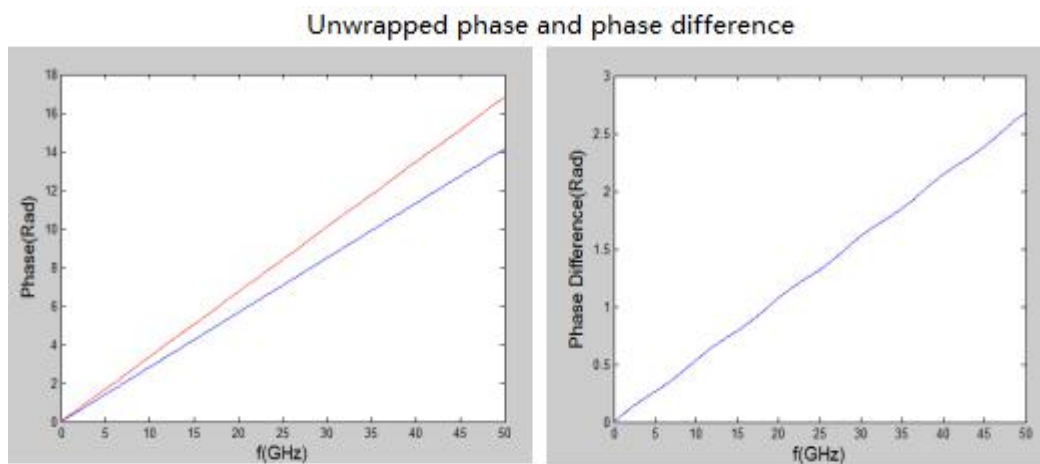


Figure 5.33. Single-ended phase (left) and phase difference (right) of the oval cross-section of the glass bundle 'worst case'

Based on formula (7) $delay = 16 \text{ ps/inch}$, the phase difference at 50 GHz is 2.7 rad.

$$delay = T \times \frac{PD}{2\pi}, \quad (7)$$

where T is the time for one period (@50GHz) and PD is the phase difference (@50GHz).

Because using the oval cross-section of the glass bundle comes with an unnecessary increase in simulation time and computational resources, the researchers prefer the previous square glass bundle model when they needed to run hundreds of simulations with different parameters.

5.2.3. Impact of Glass Weave on Jitter by DoE Method. A full wave modeling of the glass weave effect is done in HFSS. The dimensions and relative locations of the glass bundle and traces are shown in the SEM observation data in Table 5.1. Wave ports are used to excite the structure with TEM mode. Since the port should see homogeneous cross-section to excite a TEM mode, the traces are extended by 10 mils. This part will be de-embedded after simulation.

The cross-section and top view of the 5 degrees rotation non-shift model and 5 degrees rotation bundle shift model are shown in Figure 5.34.

Because in the real case, the manufacturer could not control the relative location between trace and glass bundles, most important relative location is the middle layer and bottom layer. Moreover, in every case, there are 10 shifts that are optimized and the phase

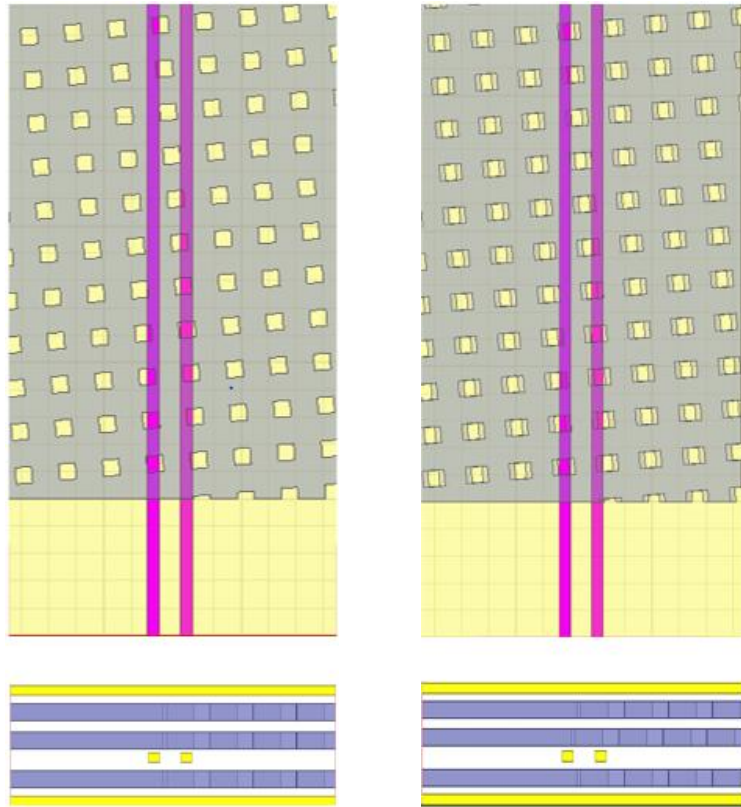


Figure 5.34. Top view and cross-section of non-bundle shift trace (left); bundle shift trace (right)

difference or jitter is the average value of 10 cases. The thickness of the glass bundle is different in the full wave model compared with the thickness in the SEM observation. To make sure the glass weave property is as close as possible to the real case, it is vital to keep the \mathcal{E}_{eff} the same. The single-ended phase and phase difference between P & N traces for both non-bundle shift case and bundle shift case are shown in Figure 5.35 and Figure 5.36. The eye diagram is shown in Figure 5.37.

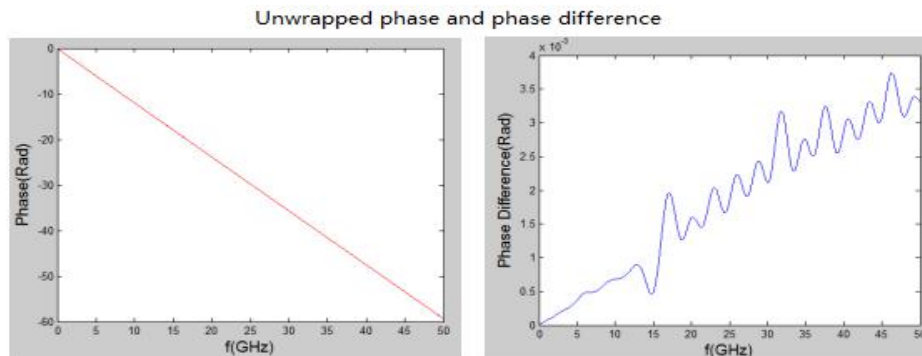


Figure 5.35. Unwrapped phase (left) and phase difference (right) of non-bundle shift case

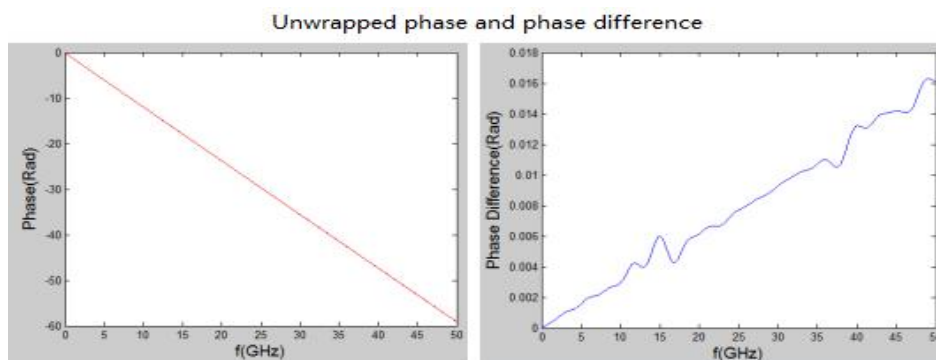


Figure 5.36. Unwrapped phase (left) and phase difference (right) of bundle shift case

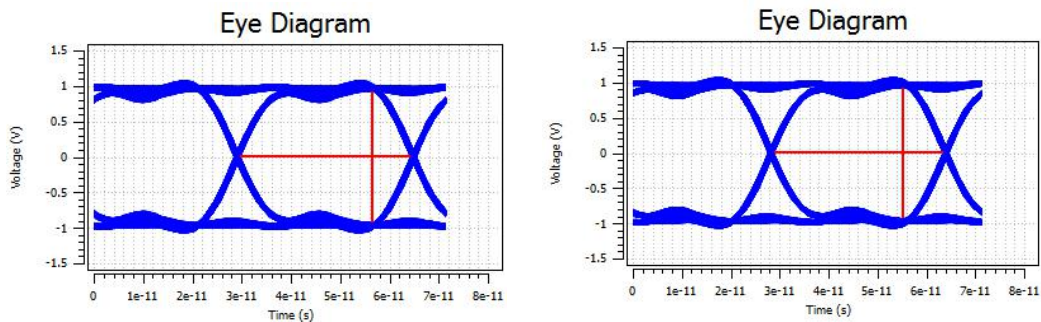


Figure 5.37. Eye diagram of non-bundle shift case (left); bundle shift case (right)

The eye-diagram were generated by FEMAS in transient mode. The source is 28 Gbps NRZ PRBS 15. After shifting the glass bundle, Sdd21 looks similar. The phase skew at 50GHz is 0.0034 rad and 0.016 rad. The jitter in the eye diagram is about 10ps.

The design of experiments (DoE) method is the design of any task that aims to describe or explain the variation of information under conditions that hypothesized to reflect the variation. In its simplest form, an experiment aims at predicting the outcome by introducing a change of the preconditions, which is represented by one or more independent variables, also referred to as “input variables”. The change in one or more independent variables is generally hypothesized to result in a change in one or more dependent variables, also referred to as “output variables”[13].

There are three kinds of input variable parameters in the full wave model. The angle of rotation is optimized from 5 degrees to 85 degrees. The schematic diagram for the angle of rotation and trace shift is shown in Figure 5.38.

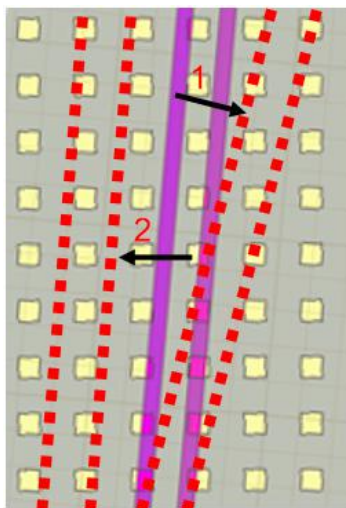


Figure 5.38. The angle of rotation and trace shift in DoE method

For each angle of rotation, the phase difference between P & N traces is calculated by the average value of trace and glass bundle shift. Thus, for each angle of rotation, the differential traces shift three times in a period. The middle layer glass bundle shifts nine times in a period. Then, the final phase difference is calculated from 27 results. The phase difference vs angle of rotation is shown in Table 5.2.

Table 5.2. Phase difference vs the angle of rotation

Angle of Rotation (degree)	Phase Difference (rad @50 GHz)	Angle of Rotation (degree)	Phase Difference (rad @50 GHz)
5	0.036	85	0.039
10	0.023	80	0.009
15	0.013	75	0.013
20	0.006	70	0.019
25	0.03	65	0.023
30	0.04	60	0.043
35	0.046	55	0.039
40	0.07	50	0.05
45	0.05		

For glass type 3313, the warp count and weft count are 61 and 62. In Table 2.1, the warp and weft bundle are almost the same, so in the DoE method, phase difference should be symmetrical for about 45 degrees. The phase difference (rad) bivariate fit by the angle of rotation is shown in Figure 5.39.

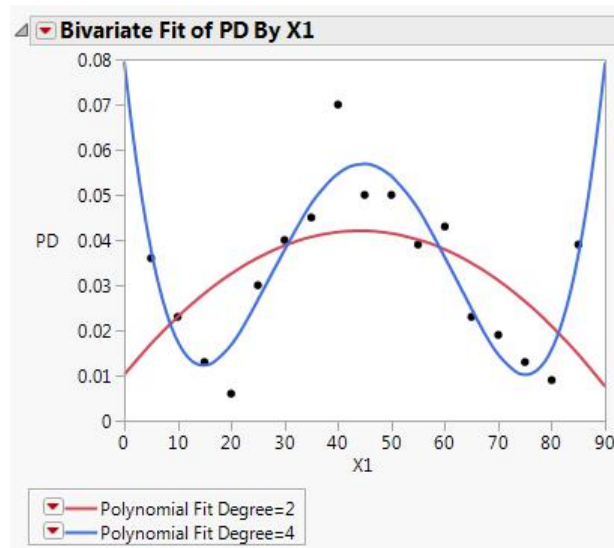


Figure 5.39. Phase difference bivariate fit by the angle of rotation

6. CONCLUSION AND FUTURE WORK

The impact of glass weave effect on differential phase skew and related methodologies are studied in this thesis. A measurement and simulation methodology to mitigate the worst case skew is presented in this work.

The full wave modeling is time confusing to get enough input and output variables of DoE method. A more robust and spanning way to instead full wave simulation, by numerical method need to be developed.

BIBLIOGRAPHY

- [1] "Impact of Fiber Weave Effect on High Speed Interconnections," *Application Note*, Caliber Interconnect Solutions.
- [2] Y. Shlepnev, C. Nwachukwu, "Modeling Skew and Jitter Induced by Fiber Weave Effect in PCB Dielectrics," *2014 IEEE International Symposium on Electromagnetic Compatibility (EMC)*, Raleigh, NC, 2014, pp. 803-808.
- [3] C. Herrick, T. Buck, R. Ding, "Bounding The Effect of Glass Weave Through Simulation," *DesignCon 2009*.
- [4] J. Miller, G. Blando, I. Novak, "Additional Trace Losses due to Glass-weave Periodic Loading," *DesignCon 2010*.
- [5] T. Zhang, "Statistical Analysis of the Fiber Weave Effect Over Differential Microstrips on Printed Circuit Boards," University of Illinois at Urbana-Champaign, 2014.
- [6] X. Tian, Y. Zhang, J. Lim, "Numerical Investigation of Glass-weave Effects on High-speed Interconnections in Printed Circuit Board," *2014 IEEE International Symposium on Electromagnetic Compatibility (EMC)*, Raleigh, NC, 2014, pp. 475-479.
- [7] A. Morgan, "Developments in Glass Yarns and Fabric Constructions," *The PCB Magazine*, March 2014.
- [8] P. Pathmanathan, P. Huray, S. Pytel, "Analytic Solutions for Periodically Loaded Transmission Line Modeling," *DesignCon 2013*.
- [9] https://en.wikipedia.org/wiki/Warp_and_weft, 28 June 2018.
- [10] "Understanding Glass Fabric," *Application Note*, Isola.
- [11] P. Pathmanathan, C. Jones, S. Pytel, "Power Loss due to Periodic Structures in High-Speed Packages and Printed Circuit Boards," *18th European Microelectronics & Packaging Conference*, UK, 2011.
- [12] G. Blando, J. Miller, I. Novak, "Attenuation in PCB Traces due to Periodic Discontinuities," *DesignCon 2006*.
- [13] https://en.wikipedia.org/wiki/Design_of_experiments, 28 June 2018
- [14] J. Miller, G. Blando, I. Novak, "Additional Trace Losses due to Glass-Weave Periodic Loading," *DesignCon 2010*.

- [15] S. McMorrow, C. Heard, "The Impact of PCB Laminate Weave on the Electrical Performance of Differential Signaling at Multi-Gigabit Data Rates," *DesignCon* 2005.
- [16] K. Nalla, "Mitigation of Glass Weave Skew Using a Combination of Low DK Spread Glass, Multi-ply Dielectric and Routing Direction", *Missouri University of Science and Technology*, 2016.
- [17] "PCB Dielectric Material Selection and Fiber Weave Effect on High-Speed Channel Routing," *Application Note*, Altera.
- [18] H. Heck, S. Hall, B. Horine, "Modeling and Mitigating AC Common Mode Conversion in Multi-Gb/s Differential Printed Circuit Boards", *DTTC* 2004 Paper.
- [19] G. Luevano, J. Shin, T. Michalka, "Practical Investigations of Fiber Weave Effects on High-speed Interfaces," *2013 IEEE 63rd Electronic Components and Technology Conference*, Las Vegas, NV, 2013, pp. 2041-2045.
- [20] T. Zhang, X. Chen, J. Schutt-Ainé, "Statistical Analysis of Fiber Weave Effect over Differential Microstrips on Printed Circuit Boards," *Signal and Power Integrity (SPI), 2014 IEEE 18th Workshop on*, Ghent, 2014, pp. 1-4. 50.
- [21] D. Bucur, "Fiber Weave Effect - a Performance-limiting factor," *Communications (COMM), 2014 10th International Conference on*, Bucharest, 2014, pp. 1-4.
- [22] S. Singh and T. Kukal, "Timing Skew Enabler Induced by Fiber Weave Effect in High Speed HDMI Channel by Angle Routing Technique in 3DFEM," *Electrical Performance of Electronic Packaging and Systems (EPEPS)*, 2015 IEEE 24th, San Jose, CA, 2015, pp. 163-166.
- [23] T. Fukumori, H. Nagaoka, D. Mizutani and M. Tani, "Simulation of Differential Skew Considering Fiber Kink Effects," *IEEE CPMT Symposium Japan 2014*, Kyoto, 2014, pp. 43-46.
- [24] A. C. Durgun and K. Aygün, "Impact of Fiber Weaves on 56 Gbps SerDes Interface in Glass Epoxy Packages," *Electrical Performance of Electronic Packaging and Systems (EPEPS)*, 2015 IEEE 24th, San Jose, CA, 2015, pp. 159-162.
- [25] Y. Cao, J. Li, J. Hu, "Design Consideration for 10 Gbps Signal Transmission Channel in Copper Backplane System," *Computational Science and Its Applications (ICCSA), 2011 International Conference on*, Santander, 2011, pp. 215-218.
- [26] A. Chada, B. Mutnury, J. Fan, "Crosstalk Impact of Periodic-Coupled Routing on Eye Opening of High-Speed Links in PCBs," in *IEEE Transactions on Electromagnetic Compatibility*, vol. 57, no. 6, pp. 1676-1689, Dec. 2015.

VITA

Feng Zhang was born in Tianjin, China in 1991. He received his Bachelor of Technology degree in Opto-electrical Information Engineering from Tianjin University (TJU), Tianjin in June 2014. He became a master's degree student in the Department of Electrical Engineering in Missouri University of Science and Technology in August 2014. He did his research at the EMC laboratory under Dr. Jun Fan. He received his Master of Science degree in Electrical Engineering from Missouri University of Science and Technology in May 2019. He worked as an intern at Gentherm Electronics from June 2017 to May 2018.